LPHE/2006–09
May 24, 2006

Phenomenological study of the doubly-rare radiative decay $B \to K^*\gamma \to K\gamma\gamma$

Mathias Knecht[*] and **Thomas Schietinger**[†]

Laboratory for High-Energy Physics (LPHE)
Ecole Polytechnique Fédérale de Lausanne (EPFL)

Abstract

We present a phenomenological study of the doubly-rare radiative decay $B \to K^*\gamma \to K\gamma\gamma$. In particular, we examine the interferences with other decays leading to the same $K\gamma\gamma$ final state, including their potential for an experimental determination of the photon polarization in $B \to K^*\gamma$ decays. (This note is the long version of a paper published in Physics Letters B 634 (2006) 403–407.)

[*]Mathias.Knecht@epfl.ch
[†]Thomas.Schietinger@cern.ch

Contents

1 Introduction

Flavour-changing neutral currents have been an important testing ground for the Standard Model (SM) of elementary particles. The quark transition $b \to s\gamma$ has played an outstanding role in this respect by providing the first direct experimental evidence for the penguin diagram process. This process is expected to be particularly sensitive to contributions from physics beyond the Standard Model, as new heavy states might appear virtually in the decay loop.

The most recent measurements of the $b \to s\gamma$ rate [1], however, agree very well with theoretical predictions [2], leaving little hope for observing hints of new physics through the decay rate only. Consequently, recent efforts have focused on finding additional observable degrees of freedom related to $b \to s\gamma$, such as CP asymmetries or the helicity of the emitted photon, in order to subject the Standard Model to ever more stringent tests.

A further possibility to increase the number of observables consists in adding a photon to the final state. The quark transition $b \to s\gamma\gamma$, to be observed inclusively via $B \to X_s\gamma\gamma$ or exclusively in channels such as $B \to K^{(*)}\gamma\gamma$ has been studied in this context [3, 4]. In analogy to $b \to sl^+l^-$, the diphoton invariant mass spectrum and forward-backward asymmetries have been suggested as probes for new physics beyond the Standard Model [5, 6]. For exclusive decays of the type $B \to K\gamma\gamma$, it was recently shown [7] that the short-distance (i.e. non-resonant) contribution to this decay is rather small, accounting for a branching fraction of the order of 10^{-9} only.

In this note, we point out the importance of contributions via radiatively decaying kaon resonances: $B \to K_{\rm res}\gamma$, with $K_{\rm res}$ being any kaon resonance such as $K^*(892)$ or higher that can decay to $K\gamma$. Due to the indistinguishability of the two photons in the final state, the decay $B \to K\gamma\gamma$ receives kaon resonance contributions via two amplitudes, $B \to K_{\rm res}\gamma_1 \to (K\gamma_2)\gamma_1$ and $B \to K_{\rm res}\gamma_2 \to (K\gamma_1)\gamma_2$. As a consequence, events due to $B \to K_{\rm res}(\to K\gamma)\gamma$ populate the entire Dalitz plot at a rate that is larger than the short-distance $B \to K\gamma\gamma$ contribution. The quark-level $b \to s\gamma\gamma$ amplitude is therefore masked everywhere by such resonance contributions and hence will remain inaccessible to experimental investigation.

Fortunately, that does not mean that $B \to K\gamma\gamma$ decays are entirely uninteresting to experimenters; quite the contrary: as we will also show in this note, the fact that decays via kaon resonances dominate across large parts of the $K\gamma\gamma$ phase space offers interesting possibilities to measure the polarization, or helicity, of the photon emitted in $B \to K^*\gamma$.

It was first pointed out by Atwood, Gronau and Soni [8] that the helicity of the photon emitted in the $b \to s\gamma$ process carries information on the interactions involved in this flavor-changing neutral current decay process. While the Standard Model amplitude for $b \to s\gamma$ results in a predominantly left-handed photon (right-handed for $\overline{b} \to \overline{s}\gamma$), there are extensions of the Standard Model which could alter the helicity of the photon without affecting much the rate of the decay. Establishing the helicity of the decay photon has thus become one of the major objectives in contemporary B physics.

Since a direct measurement of the photon helicity in radiative B decays appears to be beyond the capabilities of current experiments, several indirect methods have been devised to study this property. The methods proposed so far to analyse the decay photon fall into four categories:

- Study of the *interference between* $b \to s\gamma$ *and* $\overline{b} \to \overline{s}\gamma$: the phenomenon of B^0–$\overline{B}^0$ mixing makes this possible. The interference can be probed by measurements of time-dependent CP asymmetries [8]. If the radiated photon really is left-handed in b-decays and right-handed in $\overline{b}$-decays the interference will vanish. First measurements with the decay channels $B^0 \to K^{*0}(\to K^0_S\pi^0)\gamma$ and $B^0 \to K^0_S\pi^0\gamma$ have been reported by the BABAR and Belle collaborations [9], with results that are compatible with no interference, but statistically not yet very significant. One problem with this method to determine the photon polarization is that if the measured CP asymmetry turns out to be small, it is not immediately clear whether it is indeed the result of sizeable photon polarization or if it is due to a new phase entering the decay amplitude. But a large CP asymmetry would in any case be in conflict with the Standard Model.

- Analysis of the *decay photon by means of its conversion to a lepon pair*, i.e. study of $b \to s\gamma^{(*)}(\to \ell^+\ell^-)$. The photon may be virtual [11], $B \to K^*\ell^+\ell^-$, or real [10], $B \to K^*\gamma$, where γ converts into e^+e^- somewhere inside the detector. In both cases $K^* \to K\pi$ and the photon helicity is inferred from the angular correlation between the $K\pi$ and e^+e^- decay planes. Analysis as a function of the B meson decay time additionally gives access to the CKM parameters $\sin 2\beta$ and $\cos 2\beta$, at the cost of statistics, of course.

- Analysis of the *recoil system arising from the hadronization of the s-quark* in $b \to s\gamma$ [12, 13]. Since the two-body decay of the K^* does not provide any information on its spin orientation, this method has to resort to three-body ($K\pi\pi$) decays of higher K resonances, such as the $K_1(1400)$. Ref. [13] gives a detailed analysis of the $K\pi\pi$ resonances to be considered in the mass range 1.2–1.5 GeV. This is the most promising method for measuring the photon polarization in radiative B decays, as it can already be applied with existing data samples collected by the B factories.

- Use of a *polarized initial state* to infer the photon polarization from angular correlations with the final state. To apply this method, the b-quark obviously must be packaged in a baryon. The decay $\Lambda_b \to \Lambda\gamma$ has been suggested as a promising candidate [14, 15]. In the case where bottom baryons will be produced at a hadron collider, decays to strongly-decaying higher Λ resonances such as $\Lambda(1520)$ may be more amenable to experimental investigations [16].

There is yet another possibility to analyse the decay photon: its properties can be probed by interference with another photon, which arises from the *same decay* and is in a well-known state. The simplest example for such a situation is $B \to K^*(\to K\gamma)\gamma$ interfering with $B \to Kc\bar{c}(\to \gamma\gamma)$, where $c\bar{c}$ is a charmonium state such as η_c or χ_c. It is in this context, and with this motivation, that we present a systematic

study of the cascade decay $B \to K^*(\to K\gamma)\gamma$ and its interferences with other decays leading to the same final state $K\gamma\gamma$.

The B factories have thoroughly explored branching fractions down to 10^{-6}; the realization of so-called "Super-B factories," with expected reaches extended by yet another two orders of magnitude, is currently under discussion [17, 18], and the experiments at the Large Hadron Collider are also considering luminosity upgrades [19]. In this situation it is hardly premature to explore the physics potential of "doubly rare" decays of B mesons, i.e. rare decays in which the primary decay products themselves are observed in rare decay modes, such as $B \to K^*(\to K\gamma)\gamma$.

In Sec. 2 we review the experimental information available on $B \to K^*(\to K\gamma)\gamma$. In Sec. 3 we address the kinematics of the decay, in particular its angular distribution, before investigating, in Sec. 4, the full amplitude of the decay within the Standard Model. Section 5 summarizes other contributions to the final state $K\gamma\gamma$, which interfere with $B \to K^*(\to K\gamma)\gamma$. These interference effects are then shown to depend on the polarization of the photon emitted in $B \to K^*\gamma$ (Sec. 6), resulting in interesting experimental opportunities. We summarize our results in Sec. 7.

This note is the long version of a letter published earlier [20].

2 Experimental status of $B \to K^*\gamma$ and $K^* \to K\gamma$

The sequential decay $B \to K^*\gamma \to K\gamma\gamma$ has not yet been observed. Experimental knowledge on the subdecays allows us to estimate the effective branching fraction for the decay.

2.1 $B \to K^*\gamma$

The decay $B \to K^*\gamma$ was first observed by the CLEO collaboration [21] in the channels $K^{*0} \to K^+\pi^-$ and $K^{*+} \to K^0_S\pi^+$ and $K^+\pi^0$. The most precise branching fraction measurements to date have been obtained by the Belle [22] and BABAR [23] collaborations. The most recent averages issued by the Heavy Flavor Averaging Group [24] are

$$\mathcal{B}(B^0 \to K^{*0}\gamma) = (40.1 \pm 2.0) \times 10^{-6}, \quad (1)$$
$$\mathcal{B}(B^+ \to K^{*+}\gamma) = (40.3 \pm 2.6) \times 10^{-6}. \quad (2)$$

2.2 $K^* \to K\gamma$

The radiative decay of the K^* resonance is overwhelmed by the strong decay to $K\pi$ because of the relatively large mass difference between K^* and K. This is in contrast to the situation in the charm sector, where $D^* \to D\gamma$ represents a sizable branching fraction. Since the electromagnetic decay conserves parity, the photon is emitted in a P-wave.

The decay $K^* \to K\gamma$ has not been observed directly to date. Measurements of the radiative width are based on the observation of Primakoff production of K^* by kaon beams impinging on suitable targets.

Using a K_L beam and Cu and Pb targets, Carlsmith et al. [25] have obtained a width of 116.5 ± 9.9 keV for the K^{*0}. Comparison to the total width of the K^{*0}, $\Gamma_{\text{total}}(K^{*0}) = 50.7 \pm 0.6$ MeV [26] gives a branching fraction of

$$\mathcal{B}(K^{*0} \to K^0\gamma) = (23.0 \pm 2.0) \times 10^{-4}. \quad (3)$$

The radiative width of the charged K^* was measured at Fermilab by the E272 experiment ($K^\pm$ beams on C, Al, Cu and Pb targets). They obtained 51 ± 5 keV for the K^{*+} [27] and 48 ± 11 keV for the K^{*-} [28], which is charge-averaged to 50.5 ± 4.6 keV, corresponding to a branching fraction ($\Gamma_{\text{total}}(K^{*+}) = 50.8 \pm 0.9$ MeV [26]) of

$$\mathcal{B}(K^{*\pm} \to K^\pm\gamma) = (9.9 \pm 0.9) \times 10^{-4}. \quad (4)$$

The radiative widths of light flavor mesons, and in particular the ratios between charged and neutral decays, represent an important testing ground for quark models and symmetries and is the subject of ongoing research [29].

Both the charged and the neutral radiative width of the K^* have each been measured by a single experiment only. A direct measurement of the branching fraction at the 10% level would therefore be highly desirable. The decay $K^* \to K\gamma$

should be accessible in existing data samples from B factories, either through e^+e^- continuum production of K^* or through B and D decays to K^*X. A good candidate would be $D^0 \to K^{*-}\pi^+$ with a branching fraction of 5.9% [26].

2.3 Product branching fractions

The combination of (1) and (3) results in a product branching fraction of

$$\mathcal{B}(B^0 \to K^{*0}\gamma) \times \mathcal{B}(K^{*0} \to K^0\gamma) = (9.2 \pm 0.9) \times 10^{-8} \tag{5}$$

for the neutral channel and, with (2) and (4)

$$\mathcal{B}(B^+ \to K^{*+}\gamma) \times \mathcal{B}(K^{*+} \to K^+\gamma) = (4.0 \pm 0.4) \times 10^{-8} \tag{6}$$

for the charged one. The complete branching fraction for $B \to K\gamma\gamma$ via $K^* \to K\gamma$ is then obtained by doubling the product branching fraction to account for the exchange of the two photons, and adding (or subtracting) a possible interference term. The size of this interference term will depend on the polarization of the emitted photons. To estimate its contribution to the branching fraction, we will need the full Standard Model amplitude for the decay, see Sec. 4.

3 Kinematics of $B \to K^*\gamma \to K\gamma\gamma$ decays

3.1 Energies and momenta

In this section we will collect some useful formulae describing the kinematics of the sequential decay $B \to K^*\gamma_1$ followed by $K^* \to K\gamma_2$. Throughout this section, γ_1 will denote the primary photon, originating from the B decay, and γ_2 the secondary photon, originating from the K^* decay. For simplicity we assume a unique mass of the K^* in the decay chain, i.e. we do not take into account the effect of the finite width of that resonance. In this approximation, the photon with higher energy (as observed in the B rest frame) always originates from the first decay (the decay of the B), and therefore can by identified as γ_1 unambiguously. We will treat the more general case with interfering photons later.

It is convenient to characterise the kinematics of the decay first in the rest frame of the K^*, where all the particle energies are defined uniquely. The only free parameter is then the helicity angle θ of the second photon, defined as the angle between the momentum of the second photon γ_2 and the flight direction of the K^* (the direction opposite to the momentum of the first photon γ_1), see Fig. 1. In this reference frame, the original momentum of the decaying B meson, $\mathbf{p}_B^*$ is carried away by the first photon:

$$\mathbf{p}_B^* = \mathbf{p}_{\gamma_1}^* \tag{7}$$

(The star denotes the K^* rest frame.) Energy conservation requires

$$E_B^* = \sqrt{m_B^2 + p_B^{*2}} = m_{K^*} + p_{\gamma_1}^*, \tag{8}$$

such that ($E_\gamma = p_\gamma$)

$$E_{\gamma_1}^* = \frac{\Delta m_B^2}{2m_{K^*}}, \tag{9}$$

where we have defined $\Delta m_B^2 \equiv m_B^2 - m_{K^*}^2$. Similarly we obtain for the second decay

$$\mathbf{p}_K^* = -\mathbf{p}_{\gamma_2}^* \tag{10}$$

and

$$m_{K^*} = p_{\gamma_2}^* + \sqrt{m_K^2 + p_K^{*2}}, \tag{11}$$

which gives

$$E_{\gamma_2}^* = p_K^* = \frac{\Delta m_{K^*}^2}{2m_{K^*}}, \tag{12}$$

with $\Delta m_{K^*}^2 \equiv m_{K^*}^2 - m_K^2$. Numerically, we obtain for $m_B \approx 5.28$ GeV, $m_{K^*} \approx 0.89$ GeV, and $m_K \approx 0.50$ GeV the approximate values $E_{\gamma_1}^* \approx 15.22$ GeV and $E_{\gamma_2}^* \approx 0.30$ GeV.

It is now straightforward to obtain momenta and energies in the B rest frame by means of a Lorentz boost into that frame:

$$\begin{pmatrix} E \\ p_\parallel \end{pmatrix} = \begin{pmatrix} \gamma_B & -\beta_B\gamma_B \\ -\beta_B\gamma_B & \gamma_B \end{pmatrix} \begin{pmatrix} E^* \\ p_\parallel^* \end{pmatrix}; \qquad p_\perp = p_\perp^*, \tag{13}$$

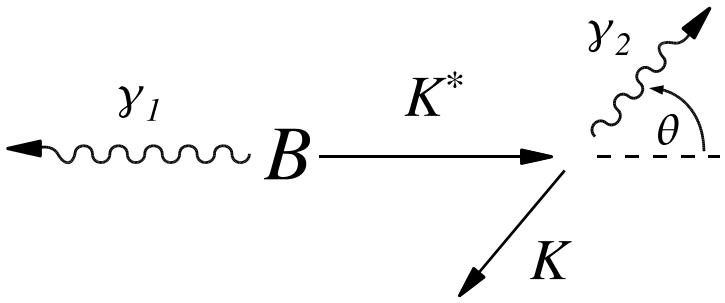

Figure 1: Kinematic definitions for the decay $B \to K^*(\to K\gamma)\gamma$. Each decay is viewed in the rest frame of the decaying particle.

with $\beta_B\gamma_B = p_B/m_B$ and $\gamma_B = \sqrt{1+(\beta_B\gamma_B)^2}$. The variables $p_\parallel$ and $p_\perp$ denote momenta parallel and perpendicular to the B momentum, respectively, and starred (unstarred) quantities refer to the K^* (B) rest frame. In our case, we obtain (dropping the B subscript of β and γ for better readability)

$$E_{\gamma_1} = (1-\beta)\gamma E^*_{\gamma_1} = \frac{\Delta m_B^2}{2m_B} \approx 2.56 \text{ GeV}, \tag{14}$$

as expected for the two-body decay $B \to K^*\gamma$. For the photon from the second decay we have

$$E_{\gamma_2} = (1+\beta\cos\theta)\gamma E^*_{\gamma_2}, \tag{15}$$

where we have used $p^*_{\parallel\gamma_2} = -p^*_{\gamma_2}\cos\theta$. The parallel and perpendicular momentum components of that photon are

$$p_{\parallel\gamma_2} = -(\cos\theta+\beta)\gamma E^*_{\gamma_2} \quad \text{and} \quad p_{\perp\gamma_2} = p^*_{\perp\gamma_2} = p^*_{\gamma_2}\sin\theta. \tag{16}$$

It is easily verified that the expression for the total momentum reproduces the photon energy,

$$p_{\gamma_2} = \sqrt{p^2_{\parallel\gamma_2} + p^2_{\perp\gamma_2}} = \sqrt{\gamma^2(\cos\theta+\beta)^2 + \sin^2\theta}\; p^*_{\gamma_2} = (1+\beta\cos\theta)\gamma p^*_{\gamma_2}. \tag{17}$$

Equations (12) and (15) define the relation between the photon helicity angle and the energy of the second photon. It may be written as

$$E_{\gamma_2} = \overline{E} + \Delta E\cos\theta \tag{18}$$

with

$$\overline{E} \equiv \frac{\Delta m^2_{K^*}}{2m_{K^*}}\sqrt{1+\left(\frac{\Delta m_B^2}{2m_B m_{K^*}}\right)^2} = E^*_{\gamma_2}\sqrt{1+\mathcal{E}^2_{\gamma_1}} \approx 0.93 \text{ GeV} \tag{19}$$

and

$$\Delta E \equiv \frac{\Delta m_B^2 \Delta m^2_{K^*}}{4m_B m^2_{K^*}} = E^*_{\gamma_2}\mathcal{E}_{\gamma_1} \approx 0.87 \text{ GeV}, \tag{20}$$

where $\mathcal{E}_{\gamma_1} \equiv E_{\gamma_1}/m_{K^*}$ is the primary photon energy expressed in units of the K^* mass. For later use, let us define in the same vein $\mathcal{E}^*_{\gamma_2} \equiv E^*_{\gamma_2}/m_{K^*}$.

From (18) we immediately obtain the minimal and maximal energies for the second photon:

$$E^{\min}_{\gamma_2} = \overline{E} - \Delta E \approx 0.05 \text{ GeV}, \qquad E^{\max}_{\gamma_2} = \overline{E} + \Delta E \approx 1.81 \text{ GeV}, \tag{21}$$

corresponding to the extreme configurations $\cos\theta = \mp 1$.

3.2 Angular distribution

Neglecting overall constants, the amplitude for a general two-body decay $\alpha \to f$ is given by [30]

$$\mathcal{A}(\alpha \to f) = D^{J*}_{M,\lambda_1-\lambda_2}(\phi_f, \theta_f, -\phi_f) A_{\lambda_1,\lambda_2} \tag{22}$$

where $D^{J*}_{M,\lambda_1-\lambda_2}$ is the usual rotation matrix element with J the total spin of the decaying particle, M its projection onto the quantization axis, and λ_1 and λ_2 the helicities of the final state particles. A_{λ_1,λ_2} is a transition amplitude independent of the decay angles and M.

In our case of the two sequential two-body decays $B \to K^*\gamma_1$ followed by $K^* \to K\gamma_2$ we obtain:

$$\begin{aligned} \mathcal{A}(M, \lambda_1, \lambda_2) \quad \propto \quad & D^{s(B)*}_{M,\lambda_1-\lambda_{K^*}}(\phi_{\gamma_1}, \theta_{\gamma_1}, -\phi_{\gamma_1}) A_{\lambda_1,\lambda_{K^*}} \\ & \times D^{s(K^*)*}_{-\lambda_{K^*},\lambda_2-\lambda_K}(\phi_{\gamma_2}, \theta_{\gamma_2}, -\phi_{\gamma_2}) B_{\lambda_2,\lambda_K}, \end{aligned} \tag{23}$$

where $\lambda_{1,2} \equiv \lambda_{\gamma_{1,2}}$ and all decay angles are defined in the rest frame of the respective decaying particle. Note that the first subscript of the second rotation matrix element $(-\lambda_{K^*})$ carries a negative sign because we choose the quantization axis of the second decay to be parallel to $\mathbf{p}_{\gamma_2}$. Now $s(B) = 0$, which implies $\lambda_1 - \lambda_{K^*} = 0$ and $\lambda_{K^*} = \lambda_1 \neq 0$. Therefore $D^{s(B)*}_{M,\lambda_1-\lambda_{K^*}} = D^{0*}_{00} = 1$. In addition we have $s(K^*) = 1$ and $\lambda_K = 0$, such that (23) simplifies to

$$\mathcal{A}(\lambda_1, \lambda_2) \propto A_{\lambda_1} D^{1*}_{-\lambda_1,\lambda_2}(\phi, \theta, -\phi) B_{\lambda_2 0}, \tag{24}$$

where we have set $\phi = \phi_{\gamma_2}$ and $\theta = \theta_{\gamma_2}$. Parity is conserved in the decay $K^* \to K\gamma$, which proceeds via the electromagnetic interaction. With the parities η of the involved particles [30] we have

$$B_{1,0} = \eta_{K^*}\eta_K\eta_\gamma(-1)^{s(K)+s(\gamma)+s(K^*)} B_{-1,-0} = -B_{-1,0}. \tag{25}$$

This means that $|B_{1,0}|^2 = |B_{-1,0}|^2$ and B will only contribute an overall factor to the transition probability. Since we are only interested in angular distributions, we may safely drop B from our calculation. Note that parity is not conserved in the first decay, $B \to K^*\gamma$, which is mediated by the weak interaction.[1]

[1] In fact, in the Standard Model we expect $|A_{1,1}|^2 \ll |A_{-1,-1}|^2$!

To obtain the angular distribution of the decay, we must sum over the photon helicities after squaring the amplitude, as they are not measured in the experiment:

$$\frac{d\Gamma}{d\cos\theta} \propto \sum_{\lambda_1,\lambda_2} |\mathcal{A}(\lambda_1,\lambda_2)|^2 = \sum_{\lambda_1,\lambda_2} |A_{\lambda_1} D^{1*}_{-\lambda_1,\lambda_2}(\phi,\theta,-\phi)|^2 = \sum_{\lambda_1,\lambda_2} |A_{\lambda_1} d^1_{-\lambda_1,\lambda_2}(\theta)|^2 \tag{26}$$

Inserting the appropriate d-functions,

$$\begin{aligned} d^1_{1,1}(\theta) = d^1_{-1,-1}(\theta) &= \frac{1+\cos\theta}{2} \quad \text{and} \\ d^1_{1,-1}(\theta) = d^1_{-1,1}(\theta) &= \frac{1-\cos\theta}{2}, \end{aligned}$$

we obtain

$$\frac{d\Gamma}{d\cos\theta} \propto (|A_1|^2 + |A_{-1}|^2)\frac{1+\cos^2\theta}{2}, \tag{27}$$

or simply

$$\frac{d\Gamma}{d\cos\theta} \propto 1+\cos^2\theta, \tag{28}$$

regardless of the value of λ_1. Thanks to (18), it is straightforward to express this distribution as a function of the secondary photon energy E_{γ_2}:

$$\frac{d\Gamma}{dE_{\gamma_2}} \propto 1 + \left(\frac{E_{\gamma_2} - \overline{E}}{\Delta E}\right)^2 \tag{29}$$

3.3 Contribution from non-sequential decays

In the limit of zero-width for the K^*, the strictly sequential decay $B \to K^*\gamma$ followed by $K^* \to K\gamma'$ is the only contribution to the final state $K\gamma\gamma'$ involving the K^* resonance, and we always have $E_\gamma > E_{\gamma'}$. If we take into account the finite width of the K^* (about 51 MeV), we find that there is a non-negligible contribution to the $K\gamma\gamma'$ final state due to the amplitude for $B \to K^*\gamma'$ followed by $K^* \to K\gamma$. If the mass of the intermediate K^* resonance—let us denote it by M_{K^*} to distinguish it from the mean mass m_{K^*}—is large enough, the photon from its decay can have a larger energy than the primary photon. The condition for this to occur can be stated as

$$E^{\max}_{\gamma_2} \geq E_{\gamma_1}, \tag{30}$$

or, using the dimensionless energies defined in Sec. 3.1

$$\mathcal{E}^{*2}_{\gamma_2} - \mathcal{E}^2_{\gamma_1}(1 - 2\mathcal{E}^*_{\gamma_2}) > 0, \tag{31}$$

where the dimensionless energies are evaluated at the resonance mass M_{K^*}. It follows that $M_{K^*} \gtrsim 1.62$ GeV.

Despite its large suppression from the Breit-Wigner resonance shape the effect of this amplitude turns out to be not negligible, because a given final state configuration $K\gamma\gamma'$ receives contributions from *both* amplitudes, $B \to K^*\gamma \to (K\gamma)\gamma'$ and $B \to$

$K^*\gamma' \to (K\gamma')\gamma$. Since we are dealing with two interfering amplitudes, the angular distribution or, in this case, the population of the $K\gamma\gamma$ Dalitz plot for these events can no longer be obtained from simple rotational symmetry arguments but must be worked out on the basis of the full decay amplitude, which we will introduce in the following section.

4 Amplitude for $B \to K^*\gamma \to K\gamma\gamma$ in the Standard Model

The Standard Model amplitude for $B \to K^*\gamma \to K\gamma\gamma$ is given in Ref. [31]. It is based on a description of the quark transition $b \to s\gamma$ in the framework of an effective Hamiltonian,

$$\mathcal{H}_{\text{eff}} = -4\frac{G_F}{\sqrt{2}} V_{tb}V_{ts}^* C_7 O_7 = -4\frac{G_F}{\sqrt{2}} V_{tb}V_{ts}^* C_7 \left(\frac{em_b}{16\pi^2}\right) \overline{s}_L \sigma_{\mu\nu} b_R F^{\mu\nu}, \tag{32}$$

with G_F the Fermi constant, C_7 the Wilson coefficient of the local operator O_7, e the electric charge, m_b the mass of the b-quark, $F^{\mu\nu}$ the electromagnetic field tensor and $\sigma_{\mu\nu} = \frac{i}{2}(\gamma_\mu\gamma_\nu - \gamma_\nu\gamma_\mu)$. V_{tb} and V_{ts} are the usual Cabibbo-Kobayashi-Maskawa (CKM) matrix elements; note that Ref. [31] writes the amplitude in terms of V_{cb} and V_{cs}, thereby utilizing the fact that $V_{cb}V_{cs}^* \approx -V_{tb}V_{ts}^*$ by virtue of the unitarity of the CKM matrix and the smallness of $V_{ub}V_{us}^*$. Note that (32) does not take into account right-handed contributions from O_7, nor contributions from operators other than O_7.

The full amplitude is then given as

$$\mathcal{M}_{K^*} = \left[T^{\mu\nu}(k_1, k_2) + T^{\nu\mu}(k_2, k_1)\right] \epsilon_\mu^*(k_1)\epsilon_\nu^*(k_2) \tag{33}$$

with

$$\begin{aligned} T^{\mu\nu}(k_1, k_2) \;=\; & \left(\frac{em_b gF}{16\pi^2}\right) 4\frac{G_F}{\sqrt{2}} V_{tb}V_{ts}^* C_7 \epsilon^{\alpha\nu\gamma\delta} k_{2\alpha}(p_B - k_1)_\gamma k_{1\beta'} \\ & \times \frac{1}{(p_B - k_1)^2 - m_{K^*}^2 + im_{K^*}\Gamma_{K^*}} \left(g_{\delta\sigma'} - \frac{(p_B - k_1)_\delta (p_B - k_1)_{\sigma'}}{m_{K^*}^2}\right) \\ & \times \left[i\epsilon^{\mu\beta'\sigma'\tau'}(p_B - k_1)_{\tau'} - \left(g^{\mu\sigma'}(p_B - k_1)^{\beta'} - g^{\beta'\sigma'}(p_B - k_1)^\mu\right)\right] \end{aligned}$$

where k_i are the 4-vectors $(E, \vec{p})$ of the photons, and p_B, p_K the 4-vectors of the B and K mesons. The constants g and F are related to the coupling strengths for $K^* \to K\gamma$ and $B \to K^*\gamma$, respectively, and are different for neutral (B^0) and charged decays (B^+). Eq. 33 is consistent with the amplitude quoted in Ref. [32].

To illustrate the kinematic distributions resulting from this amplitude, we generate decays using the `EvtGen` package [33], the Monte Carlo event generation software of choice of, among others, the B factory experiments Belle and BABAR as well as LHCb. For implementation details, we refer to Ref. [34]. Figure 2 shows the Dalitz plot for 100 000 generated events, in the plane of the two photon energies. The accumulations at the resonance energies $E_\gamma \approx 2.56$ GeV (see Eq. 14) are well visible on both axes, and exhibit the expected angular distribution (29). Also visible is the sizeable contribution from the non-sequential decays (see Sec. 3.3) in the central bulk of the Dalitz plot.

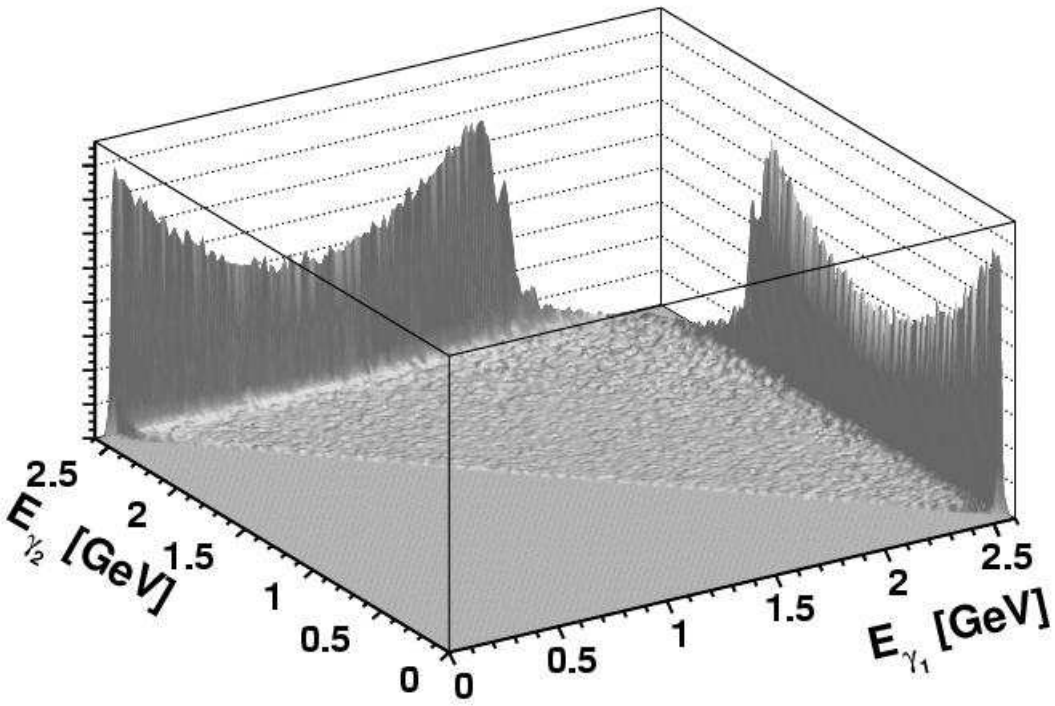

Figure 2: Dalitz plot in the plane of the two photon energies.

4.1 Estimate of the effective $B \to K^*\gamma \to K\gamma\gamma$ branching fraction

The distribution of events obtained from the amplitude (33) allows us to estimate the size of the interference term and hence the total size of the $B \to K\gamma\gamma$ branching fraction due to $K^* \to K\gamma$. A comparison of the decay distribution obtained from a strictly sequential decay chain $B \to K^*\gamma, K^* \to K\gamma$ with that computed using the full amplitude $B \to K^*\gamma \to K\gamma\gamma$ according to (33) shows that the total branching fraction to $K\gamma\gamma$ due to the K^* contribution is substantially larger than the product branching fraction. We find

$$\mathcal{B}(B \to K^*\gamma \to K\gamma\gamma) \approx 3.85 \times \mathcal{B}(B \to K^*\gamma) \times \mathcal{B}(K^* \to K\gamma). \tag{34}$$

This estimate does not take into account interferences with other amplitudes leading to the $K\gamma\gamma$ final state (see Sec. 5). Based on (5) and (6) we arrive at the following estimates for the total effective branching fractions:

$$\mathcal{B}(B^0 \to K^{*0}\gamma \to K^0\gamma\gamma) \approx (3.54 \pm 0.35) \times 10^{-7}, \tag{35}$$
$$\mathcal{B}(B^+ \to K^{*+}\gamma \to K^+\gamma\gamma) \approx (1.54 \pm 0.15) \times 10^{-7}. \tag{36}$$

These branching fractions should be well accessible with the next generation of B factories (Super B factories) and may be accessible at hadron collider experiments

if backgrounds can be controlled. We will later see (Sec. 5.2) that other kaon resonances contribute at similar levels to the same final state, thus raising the total $B \to K\gamma\gamma$ branching fraction to a level that may even be observable at currently running B factories.

4.2 Relevance of non-sequential decays

The interference term can lead to surprising distributions in other variables. Figure 3 shows the distribution of the invariant mass of the kaon and the softer of the two photons. According to our (naive) kinematic considerations in Sec. 3, we would expect the softer photon to originate *always* from the $K^* \to K\gamma$ decay and thus to follow a Breit-Wigner curve together with the kaon. Instead we find that in a sizeable fraction of the events, the soft photon apparently cannot be associated directly with the K^* decay, giving rise to a tail in the invariant mass distribution.

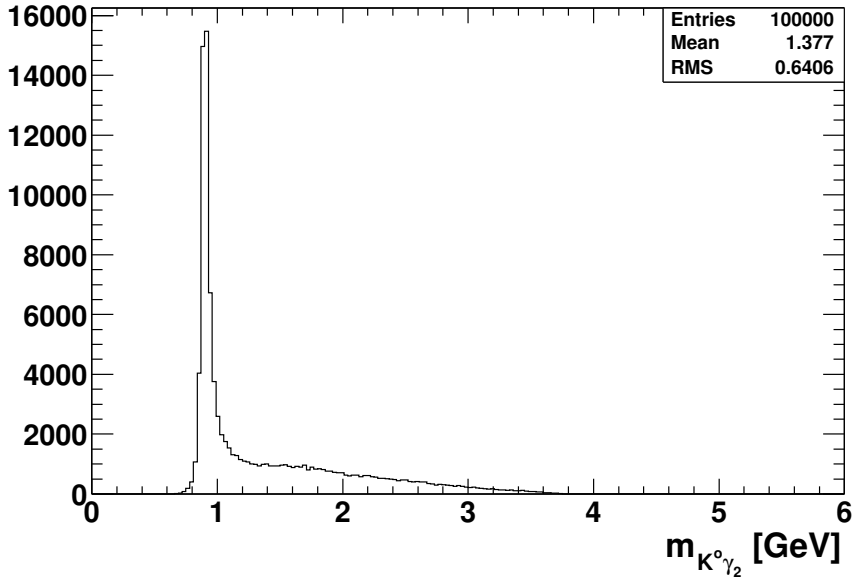

Figure 3: Distribution of the invariant mass of the kaon and the softer photon.

Another important consequence of the events due to the interference term is that they may not a priori be neglected in calculations of "hard" $B \to K\gamma\gamma$ decays (see Sec. 5.4). In a recently published calculation [7], Hiller and Safir apply the operator product expansion (OPE) technique to estimate the branching fraction of $B \to K\gamma\gamma$ in a limited region of phase space, where such an expansion is valid. They define an "OPE region" with boundaries given by $E_{1,2} < 2$ GeV and $q^2 = (k_1 + k_2)^2 > m_B/5$ that ensures high virtuality of the internal s- and b-quark lines and thus the applicability of the OPE. Based on the Standard Model amplitude (33) we obtain that about 3.2% of all $B \to K^*\gamma \to K\gamma\gamma$ decays will fall into this OPE region. Assuming a total branching fraction of 3.5×10^{-7} for $B \to K^*\gamma \to K\gamma\gamma$ (neutral case, Eq. 35), we get that $\mathrm{BR}(B \to K^*\gamma \to K\gamma\gamma|_{\mathrm{OPE}}) \approx 1.1 \times 10^{-8}$, an order of

magnitude larger than the value obtained for the Standard Model short-distance contribution in Ref. [7]!

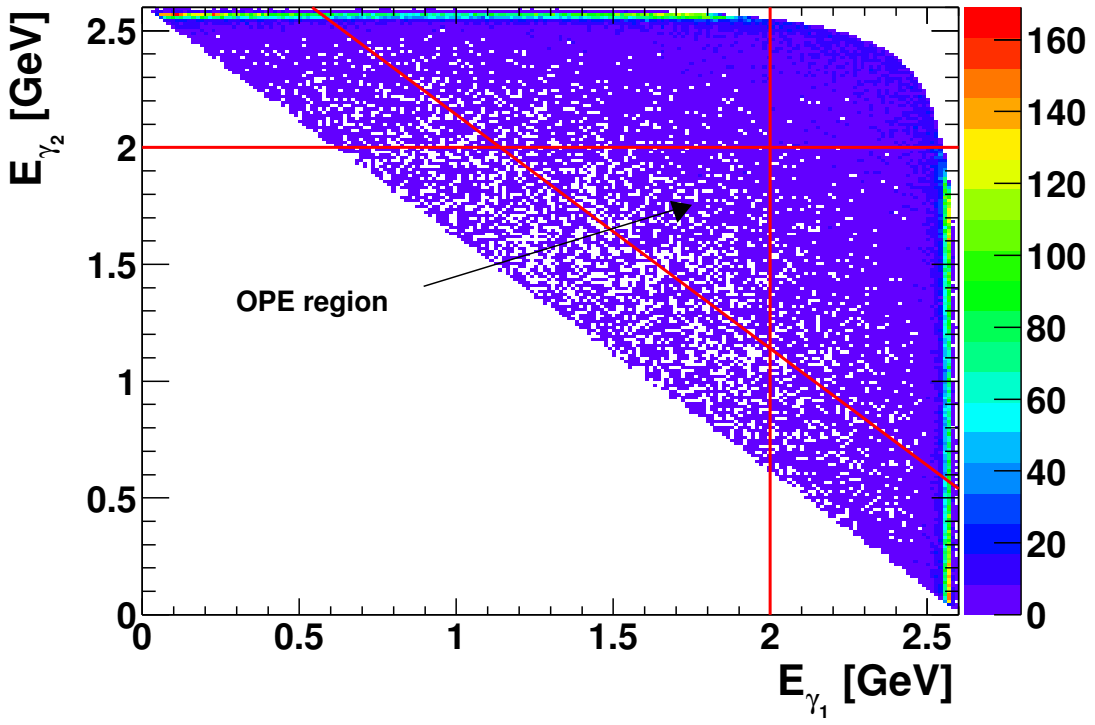

Figure 4: Dalitz plot as in Fig. 2, with the boundaries of the "OPE region" defined in Ref. [7] shown as red lines.

We conclude this section by showing another spectrum of importance for the following phenomenological analysis, the distribution of the diphoton invariant mass (Fig. 5). It peaks around 4.25 GeV/c^2.

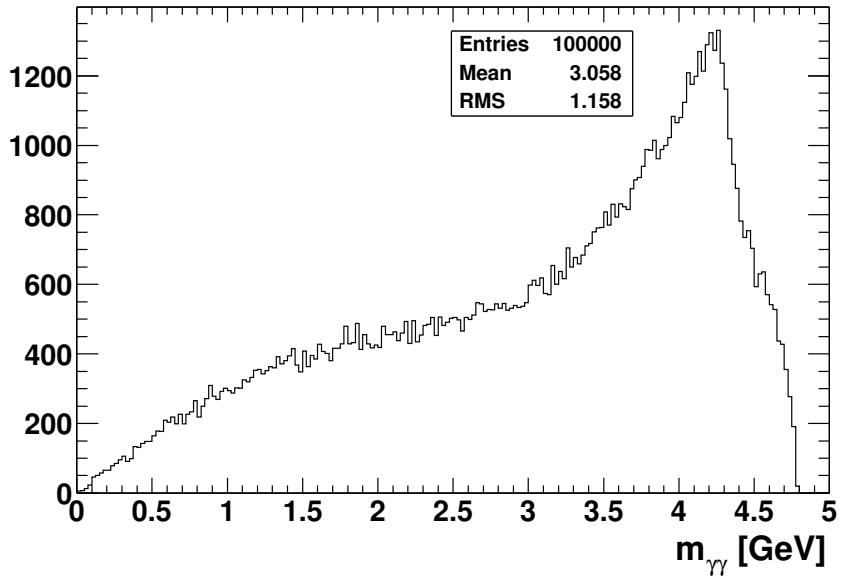

Figure 5: Diphoton invariant mass spectrum for $B \to K^*\gamma \to K\gamma\gamma$ events

5 Other contributions to the $K\gamma\gamma$ final state

In this section we examine other possible intermediate states that can yield the same $K\gamma\gamma$ final state in B decays, in order to explore the physics potential of $B \to K^*\gamma \to K\gamma\gamma$ decays. Our aim is, on the one hand, the identification of amplitudes yielding photons in well-defined polarization states, such that their interference with $B \to K^*\gamma \to K\gamma\gamma$ will contain information on the polarization of the photon emitted in the $b \to s\gamma$ transition. On the other hand, we need to know all other processes that could also result in $K\gamma\gamma$ and pollute or even mask such interference effects, and hence impair the polarization measurement.

Besides $B \to K^*\gamma \to K\gamma\gamma$, the contributions to the $K\gamma\gamma$ final state can be split into four categories:

- contributions from $\eta \to \gamma\gamma$ and $\eta' \to \gamma\gamma$;
- contributions from higher kaon resonances decaying to $K\gamma$;
- contributions from charmonium resonances decaying to $\gamma\gamma$;
- non-resonant $K\gamma\gamma$ contribution.

In the following we review the experimental and theoretical information available on these contributions. We do not consider the contribution from $\pi^0 \to \gamma\gamma$ as it does not interfere with the other contributions to $K\gamma\gamma$ due to the finite decay length of the π^0. For those channels that will be relevant to our investigations concerning the photon polarization measurement, we cite the amplitude formulae necessary for a detailed numerical evaluation of the contribution.

5.1 Contributions from η and η'

The contributions from $B \to K\eta^{(\prime)} \to K\gamma\gamma$ are mostly well established experimentally. The $\gamma\gamma$ branching fractions of η and η' are known to be $39.43 \pm 0.26\%$ and $2.12 \pm 0.14\%$, respectively [26]. Combined with the latest averages and limits for the B decays [24] we obtain the branching fractions listed in Table 1. The large $B \to K\eta'$ rate is largely compensated by the smaller $\eta' \to \gamma\gamma$ branching fraction. The cascade decay $B^+ \to K^+\eta \to K\gamma\gamma$ has been directly observed by both Belle and BABAR.

In the context of $B \to K\gamma\gamma$ these decays have been studied in Ref. [31]. Due to the tiny width of the η, $\Gamma_\eta = 1.29 \pm 0.07$ keV, there is very little interference with $B \to K^*\gamma \to K\gamma\gamma$. The η' contribution ($\Gamma_{\eta'} = 202 \pm 16$ keV) features appreciable interference with $B \to K^*\gamma \to K\gamma\gamma$, thanks to its somewhat larger width and effective branching fraction, and could in principle be used to determine the $b \to s\gamma$ photon polarization in a similar way as the η_c. Nevertheless, its small width and low diphoton mass in a region where the $B \to K^*\gamma \to K\gamma\gamma$ contribution is relatively small (see Fig. 5) and experimental backgrounds are expected to be large, make it a much less suitable candidate to illustrate our method. We therefore do not discuss the η and η' contributions any further.

Table 1: Branching fractions for the cascade decays $B \to K\eta^{(\prime)}(\to \gamma\gamma)$. The values for $\mathcal{B}(B \to K\eta^{(\prime)})$ are taken from Ref. [24] and are based on Ref. [35].

Mode	$\mathcal{B}(B \to K\eta^{(\prime)})$ (10^{-6})	$\mathcal{B}(B \to K\eta^{(\prime)} \to K\gamma\gamma)$ (10^{-6})
$B^0 \to K^0\eta \to K^0\gamma\gamma$	< 2.0	< 0.8
$B^+ \to K^+\eta \to K^+\gamma\gamma$	2.6 ± 0.5	1.0 ± 0.2
$B^0 \to K^0\eta' \to K^0\gamma\gamma$	68.6 ± 4.2	1.45 ± 0.09
$B^+ \to K^+\eta' \to K^+\gamma\gamma$	70.8 ± 3.4	1.50 ± 0.07

5.2 Contributions from higher kaon resonances

Higher kaon resonances can also decay to $K\gamma$ and thus contribute to the $K\gamma\gamma$ final state. While the radiative width of the $K_2^*(1430)^+$ has been known for quite some time [36], the KTeV collaboration has recently published measurements for $K_1(1270)^0$ and $K_1(1400)^0$ as well as upper limits for $K^*(1410)^0$ and $K_2^*(1430)^0$. Corresponding radiative B decays to these resonances have been observed for $K_1(1270)^+$, $K_2^*(1430)^0$, and $K_2^*(1430)^+$ [37]. Table 2 summarizes the experimental situation. The available information suggests that a number of kaon resonances contribute to this final state, thus raising the total $B \to K\gamma\gamma$ branching fraction due to kaon resonances possibly by an order of magnitude with respect to (35,36), bringing it to a level that may even be accessible at currently running B factories.

Table 2: Summary of the experimental information available on $B \to K_{\rm res}\gamma$ and $K_{\rm res} \to K\gamma$ [24, 26, 36, 38, 37]. For comparison we repeat the figures for $K^*(892)$ from Sec. 2.

Resonance $K_{\rm res}$	$\mathcal{B}(B \to K_{\rm res}\gamma)$ (10^{-6})	$\Gamma_{K_{\rm res}}(K\gamma)$ [keV]	$\mathcal{B}(B \to K_{\rm res}\gamma) \times \mathcal{B}(K_{\rm res} \to K\gamma)$ (10^{-8})
$K_1(1270)^0$	–	73 ± 29	$\approx 3.5^a$
$K_1(1270)^+$	42.8 ± 10.3	–	–
$K_1(1400)^0$	–	281 ± 47	$< 2.3^a$
$K_1(1400)^+$	< 14.4	–	–
$K^*(1410)^0$	< 130	< 53	< 3
$K^*(1410)^+$	–	–	–
$K_2^*(1430)^0$	12.4 ± 2.4	< 5.4	< 0.06
$K_2^*(1430)^+$	14.5 ± 4.3	240 ± 45	≈ 3.5
$K^*(892)^0$	40.1 ± 2.0	116.5 ± 9.9	9.2 ± 0.9
$K^*(892)^+$	40.3 ± 2.6	50.5 ± 4.6	4.0 ± 0.4

[a] Assuming isospin invariance for the $B \to K_{\rm res}\gamma$ decay.

The phenomenology of these decays with respect to interference with charmonium resonances as a function of photon polarization can be analyzed in a manner similar to the case $B \to K^*\gamma \to K\gamma\gamma$. In view of the coarse experimental informa-

tion available on these contributions, we leave them to future investigations.

5.3 Charmonium contributions

A substantial contribution to the $K\gamma\gamma$ final state is to be expected from charmonium states, since B meson decays to charmonium are not Cabibbo-suppressed. The charmonium states η_c, χ_{c0}, and χ_{c2} are known to decay into two photons. The decay $B \to \eta_c K$ was found by CLEO [39] and confirmed by Belle [40], with branching fractions in the expected range. The decay $B \to \chi_{c0} K$ is forbidden in the naive factorization approximation and its observation at a rather high rate by Belle [41] therefore came as a surprise. In the meantime BABAR have confirmed the decay at a branching fraction that is somewhat smaller than, but in accordance with, the Belle result [42], bringing the average decay rate in agreement with recent estimates taking into account vertex and spectator corrections [43]. Rather tight limits have been set on $B \to \chi_{c2} K$, thus excluding the rescattering mechanism as an explanation for the $\chi_{c0} K$ enhancement. Table 3 gives an overview of the expected charmonium contributions to $K\gamma\gamma$ based on available branching fraction measurements.

Table 3: Branching fractions for the cascade decays $B \to K(c\bar{c}) \to K\gamma\gamma$, where $(c\bar{c}) = \eta_c, \eta_c', \chi_{c0}, \chi_{c2}$, as far as they have been measured [26, 41, 42, 44].

Mode	$\mathcal{B}(B \to K(c\bar{c}))$ (10^{-4})	$\mathcal{B}((c\bar{c}) \to \gamma\gamma)$ (10^{-4})	$\mathcal{B}(B \to K(c\bar{c}) \to K\gamma\gamma)$ (10^{-7})
$B^0 \to K^0\eta_c \to K^0\gamma\gamma$	12 ± 4	4.3 ± 1.5	5.2 ± 2.5
$B^+ \to K^+\eta_c \to K^+\gamma\gamma$	9.0 ± 2.7	4.3 ± 1.5	3.9 ± 1.8
$B^0 \to K^0\chi_{c0} \to K^0\gamma\gamma$	< 5	2.6 ± 0.5	< 1.3
$B^+ \to K^+\chi_{c0} \to K^+\gamma\gamma$	3.0 ± 0.7	2.6 ± 0.5	0.8 ± 0.2
$B^0 \to K^0\chi_{c2} \to K^0\gamma\gamma$	< 0.41	2.46 ± 0.23	< 0.10
$B^+ \to K^+\chi_{c2} \to K^+\gamma\gamma$	< 0.30	2.46 ± 0.23	< 0.07
$B^0 \to K^0\eta_c' \to K^0\gamma\gamma$	≈ 5 (?)[a]	–	–
$B^+ \to K^+\eta_c' \to K^+\gamma\gamma$	≈ 3 (?)[a]	–	–

[a] Estimate based on [44] assuming $\mathcal{B}(\eta_c' \to K_S K^- \pi^+) = \mathcal{B}(\eta_c \to K_S K^- \pi^+)$.

As will become clear later, the charmonium contributions via η_c and χ_{c0} are the best candidates for an indirect determination of the $b \to s\gamma$ photon polarization measurement involving decay interferences. Since we will use these decays for quantitative estimates later, we give here the explicit Standard Model amplitudes for these contributions.

5.3.1 η_c contribution

The amplitude for the decay $B \to K\eta_c(\gamma\gamma)$ was worked out in Ref. [31] within the factorization approximation:

$$\begin{aligned}\mathcal{M}_{\eta_c} &= 2B_{\eta_c} f_{\eta_c} \frac{G_F}{\sqrt{2}} V_{tb} V_{ts}^* \left(C_1 + \frac{C_2}{3}\right) F_0^{BK}(m_{\eta_c}^2)(m_B^2 - m_K^2) \\ &\times \epsilon^{*\mu}(k_1)\epsilon^{*\nu}(k_2)\ \epsilon_{\mu\nu\alpha\beta} k_1^\alpha k_2^\beta\ \frac{1}{q^2 - m_{\eta_c}^2 + i m_{\eta_c}\Gamma_{\eta_c}}\end{aligned}$$

Here, B_{η_c} parameterizes the $\eta_c \to \gamma\gamma$ decay rate, f_{η_c} describes the η_c coupling to the vacuum state, and $F_0^{BK}(m_{\eta_c}^2)$ is a $B \to K$ form factor. The Wilson coefficients C_1 and C_2 are associated with the operators O_1 and O_2, respectively, and as usual $q^2 = (k_1 + k_2)^2$ with k_1 and k_2 the four-momenta of the two photons.

Figure 6 shows the decay distribution (Dalitz plot) in the plane of the two photon energies obtained from this amplitude. It exhibits the expected diagonal along which the diphoton mass equals the η_c mass, $q^2 = m_{\eta_c}^2$.

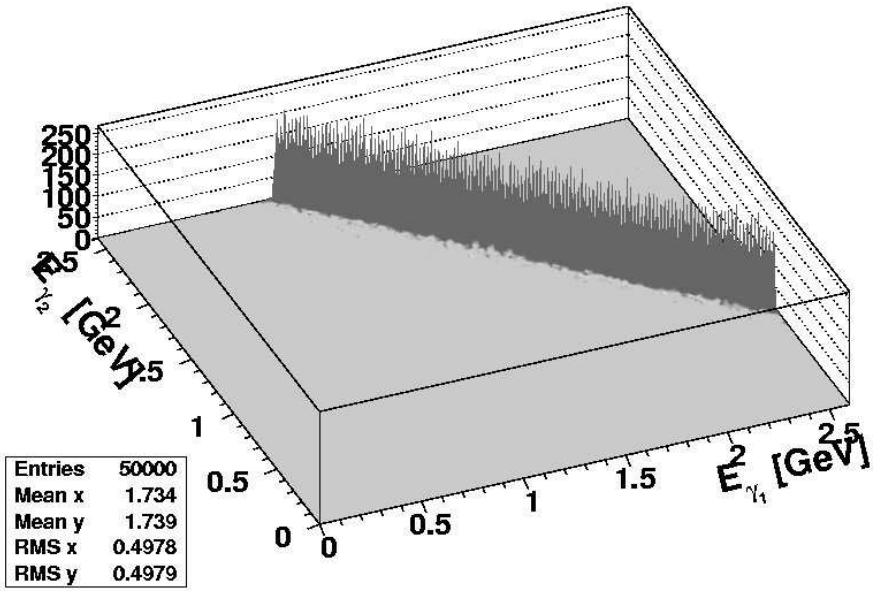

Figure 6: Dalitz plot in the plane of the two photons energies for the η_c contribution.

5.3.2 χ_{c0} contribution

Since the factorization approximation is not valid in this case, we use a general Breit-Wigner Ansatz along the lines described in Ref. [7] to compute the $B \to \chi_{c0}K$ amplitude:

$$\mathcal{A}(B \to K(\chi_{c0} \to \gamma\gamma)) = \frac{\mathcal{A}(B \to K\chi_{c0}) \times \mathcal{A}(\chi_{c0} \to \gamma\gamma)}{q^2 - m_{\chi_{c0}}^2 + i m_{\chi_{c0}}\Gamma_{\chi_{c0}}} \tag{37}$$

with

$$\mathcal{A}(\chi_{c0} \to \gamma\gamma) = a(\chi_{c0}) F_{\mu\nu} F^{\mu\nu} \tag{38}$$

where $|a(\chi_c^0)|$ is to be determined from the observed decay rate, and $F^{\mu\nu}$ denotes the electromagnetic field tensor.

$F_{\mu\nu}F^{\mu\nu}$ is even under CP and we may write

$$F_{\mu\nu}F^{\mu\nu} \propto (k_1 \cdot k_2)\epsilon^{*\mu}(k_1)\epsilon^{*\nu}(k_2)\left(g_{\mu\nu} - \frac{k_{2\mu}k_{1\nu}}{k_1 \cdot k_2}\right) \tag{39}$$

We can therefore write the complete amplitude as

$$\mathcal{M}_{\chi_{c0}} \;=\; -i\; b(\chi_{c0})(k_1 \cdot k_2)\left(g_{\mu\nu} - \frac{k_{2\mu}k_{1\nu}}{k_1 \cdot k_2}\right) \frac{\epsilon^{*\mu}(k_1)\epsilon^{*\nu}(k_2)}{q^2 - m^2_{\chi_{c0}} + i m_{\chi_{c0}}\Gamma_{\chi_{c0}}}$$

with $|b(\chi_{c0})|$ to be determined from the measured rates $\Gamma(B \to K\chi_{c0})$ and $\Gamma(\chi_{c0} \to \gamma\gamma)$. It should be noted that in this simplified parameterization we neglect any variations in the amplitude beyond the Breit-Wigner form.

The Dalitz plot for the $B \to \chi_{c0}K$ contribution (Fig. 7) is completely analog to the η_c contribution (Fig. 6).

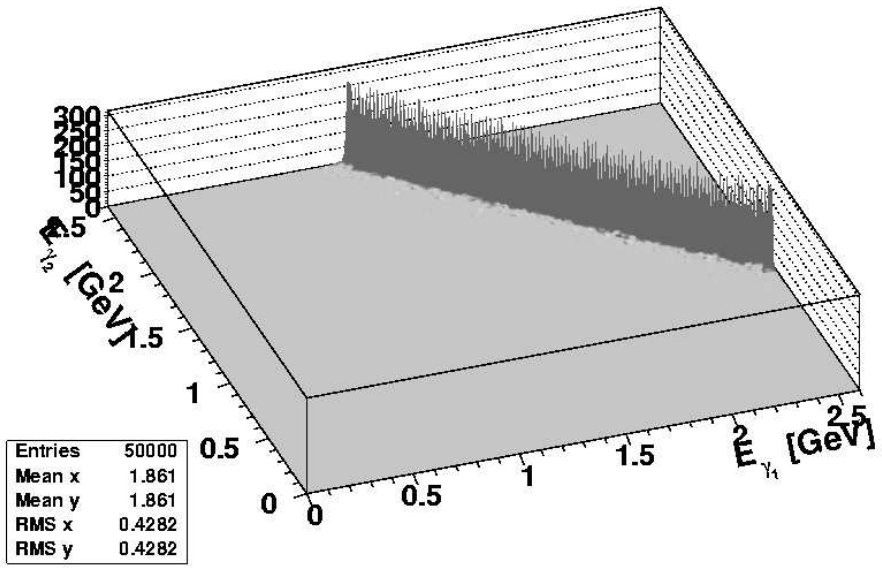

Figure 7: Dalitz plot in the plane of the two photons energies for the χ_{c0} contribution.

5.4 Non-resonant contribution

Charged and neutral B mesons can also directly decay to the final state $K\gamma\gamma$. At the quark level, the associated amplitude can be split into a reducible part, where one of the photons is emitted from an external quark line of the $b \to s\gamma$ decay, and

an irreducible part, where both photons are emitted directly from an internal quark loop [32, 31, 7]. The contribution from the reducible part is non-local, rendering the calculation difficult. Fortunately, it is strongly suppressed at the hadron level because $B \to K\gamma$ is forbidden by virtue of angular momentum conservation. The reducible part of the amplitude is controlled either by absorbing it completely into resonant contributions [32, 31], or by restricting the calculation to a kinematical region that guarantees the high virtuality of the internal s- and b-quark lines ("OPE-region", see Sec. 4), where the contribution from the reducible amplitude is bound to be small.

Using the amplitude given in [31] we obtain the Dalitz plot shown in Fig. 8, and the distribution in $q^2 = (k_1 + k_2)^2$ given in Fig. 9. The latter distribution agrees well with the one given in Fig. 4 of Ref. [7] for the Standard Model short-distance contribution. It should be noted, however, that in our distribution, no kinematical requirements are imposed. The different position of the edge (8 versus 9 GeV^2 in [7]) can be ascribed to a different numerical value for the charm quark mass.

By comparing the non-resonant amplitude with the amplitude for $B \to K^*\gamma \to K\gamma\gamma$, Eq. (33), we find that the contribution to the branching fraction of the former only amounts to a few percent of the contribution of the latter. In other words, the non-resonant contribution to the branching fraction turns out to be of the order of 10^{-9}. Our evaluation of the amplitudes given by Choudhury et al. [31] thus confirms the small non-resonant branching fraction that was first reported by Hiller and Safir [7] in contradiction to Choudhury et al.'s own value. Choudhury et al. have recently acknowledged a numerical error in their computations and published an updated value in accordance with Hiller and Safir [45].

In summary, the non-resonant $B \to K\gamma\gamma$ background to $B \to K^*\gamma \to K\gamma\gamma$ is smaller by about an order of magnitude everywhere in phase space and may be neglected when studying interference effects between $B \to K^*\gamma \to K\gamma\gamma$ and $B \to K\gamma\gamma$ via charmonium resonances.

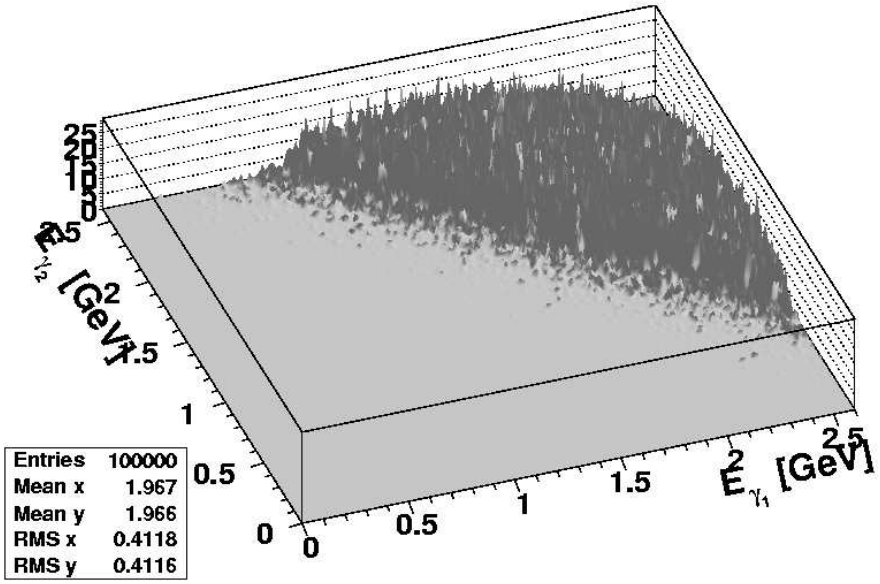

Figure 8: Dalitz plot for the irreducible contribution

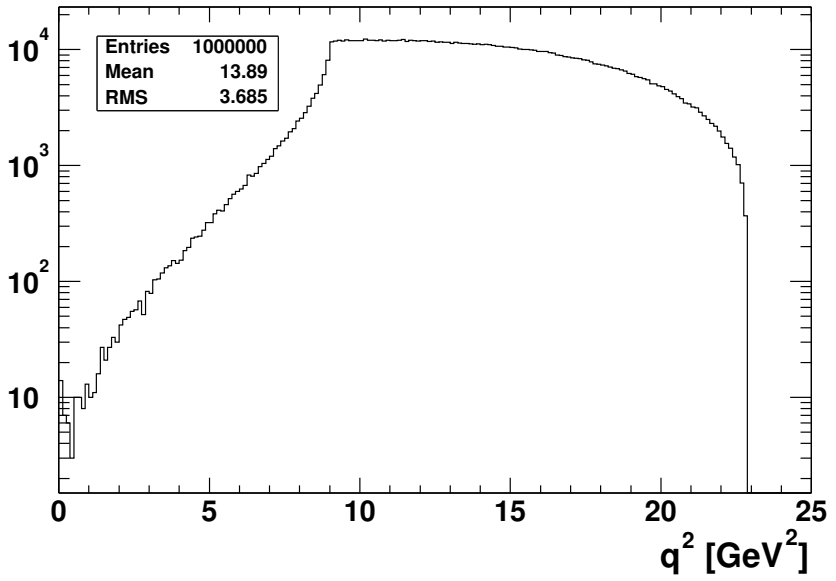

Figure 9: Non-resonant contribution to $B \to K\gamma\gamma$ as a function of $q^2 = (k_1 + k_2)^2$.

5.5 Interference effects

Leaving aside the poorly known contributions from higher kaon resonances as well as the $\eta(')$ contributions at small diphoton masses, the $B \to K\gamma\gamma$ amplitude reads

$$\mathcal{A}(B \to K\gamma\gamma) = \mathcal{A}_{\text{non-res}} + \xi_{K^*}\mathcal{A}_{K^*} + \mathcal{A}_{\eta_c} + \xi_{\chi_{c0}}\mathcal{A}_{\chi_{c0}}, \tag{40}$$

where $\xi_{K^*,\chi_{c0}} = \pm 1$ denote the signs of the respective interference terms. The sign of the η_c term is known to be positive from general unitarity considerations [4, 46] (Ref. [31] invokes the anomaly equation). Unfortunately, the same argument appears to be invalid for the χ_{c0} contribution. Likewise, the sign (phase) of the K^*-term remains unknown as pointed out in Ref. [32].

Note that in our simplified approach within the factorization approximation we are neglecting the effect of relative strong phases between the $B \to K^*\gamma$ and $B \to \eta_c(\chi_{c0})K$ decays, i.e., we assume that the $\xi_{K^*,\chi_{c0}}$ are indeed mere signs. Recent evaluations for $B \to D\pi$ [47] and $B \to \pi\pi$ [48], however, indicate sizable strong phases, thus casting into doubt this assumption. For the rest of this note, however, we assume negligible strong phases and refer to our letter [20] for a brief discussion of the issue.

Figure 10 shows the Dalitz plot corresponding to (40), with positive interference signs assumed everywhere, and amplitude strengths adjusted to the effective branching fractions inferred from experimental data. In Fig. 11 we show the corresponding diphoton invariant mass spectrum.

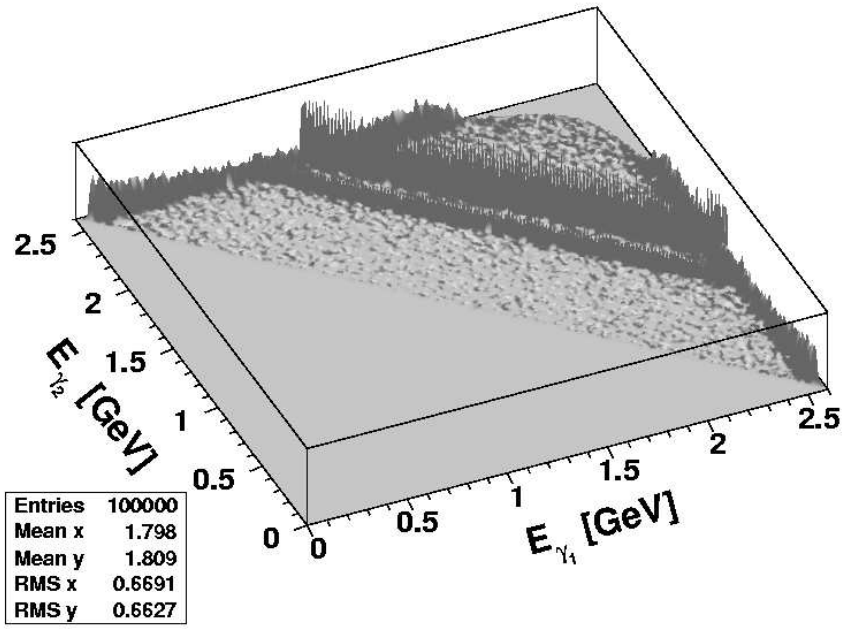

Figure 10: Dalitz plot showing the sum of all the contributions with interference terms.

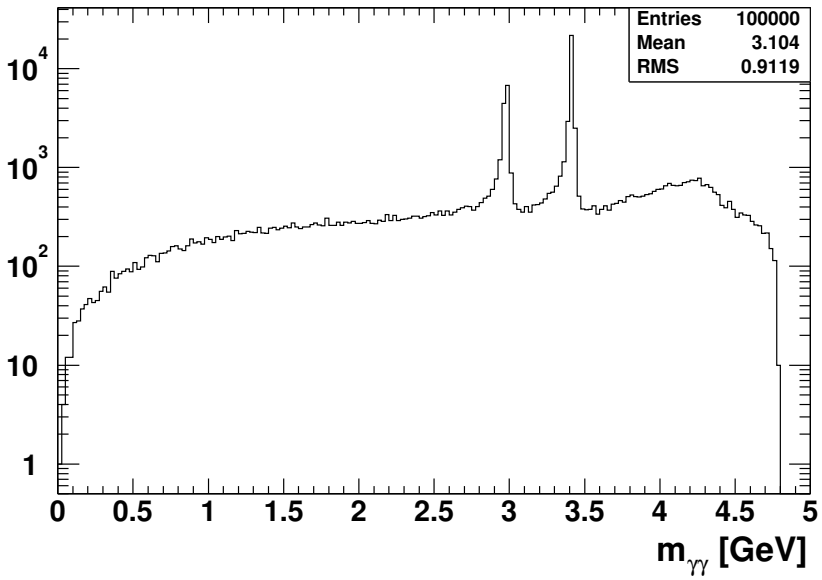

Figure 11: Diphoton invariant mass spectrum for all contributions, including interference terms.

6 Sensitivity to the photon polarization

6.1 General considerations

The interference of $B \to K^*\gamma \to K\gamma\gamma$ with other decays yielding the same $K\gamma\gamma$ final state offers interesting experimental opportunities. In particular, the interference with amplitudes proceeding via charmonium resonance states, which produce photon pairs in well-defined states, gives a handle for ascertaining the polarisation state of the photons from $B \to K^*\gamma \to K\gamma\gamma$. This is because the interference can only occur for equal, i.e. indistinguishable, polarization states of the two photons.

If the $B \to K^*\gamma$ decay predominantly results in a left-handed photon, as is expected in the Standard Model, then the polarization state of the two photons in the $K\gamma\gamma$ final state will be a superposition of parallel, perpendicular and mixed left-right circularly polarized state, depending on the kinematical configuration of the three decay products.

On the other hand, photon pairs arising from η_c ($J^P = 0^-$) decay are known to be in an exact state of perpendicular polarization [49], i.e. a state with photon spin orientation arising from a matrix element proportional to $\mathbf{k_1} \cdot [\boldsymbol{\epsilon_1}(\mathbf{k_1}) \times \boldsymbol{\epsilon_2}(\mathbf{k_2})]$, where $\boldsymbol{\epsilon_1}$ and $\boldsymbol{\epsilon_2}$ ($\mathbf{k_1}$ and $\mathbf{k_2}$) are the transverse polarization (momentum) vectors of the two photons. This corresponds to a Lorentz-invariant amplitude proportional to $F^{\mu\nu}\tilde{F}_{\mu\nu}$, odd under parity P but even under charge conjugation C (as usual, $\tilde{F}_{\mu\nu} = \frac{1}{2}\epsilon^{\mu\nu\alpha\beta}F_{\mu\nu}$). Similarly, photons from χ_{c0} ($J^P = 0^+$) decay are in a state of parallel polarisation (matrix element proportional to $\boldsymbol{\epsilon_1}(\mathbf{k_1}) \cdot \boldsymbol{\epsilon_2}(\mathbf{k_2})$), with amplitude $\propto F^{\mu\nu}F_{\mu\nu}$, which is even under P and C.

Thus we may use η_c and χ_{c0} as probes to analyze the polarization state of the photons from $B \to K^*\gamma \to K\gamma\gamma$. The photons from η_c will only interfere with the perpendicular polarisation component whereas the photons from χ_{c0} will only interfere with the parallel component. The combined information from the measurable interference patterns can then be used to determine the helicity of the photon in $B \to K^*\gamma$, an important test of the Standard Model. In the following sections, we will have a more detailed look at the interference terms at play.

6.2 Right-handed photon amplitude in $B \to K^*\gamma$

In order to study the dependence of the above-mentioned interference terms we generalize the Standard Model amplitude for $B \to K^*\gamma \to K\gamma\gamma$ to include an amplitude for the emission of a right-handed photon from the b-quark. Following Ref. [13], we complement the operator O_7 from Eq. 32 with a right-handed part,

$$C_7 O_7 = C_{7L} O_{7L} + C_{7R} O_{7R} \tag{41}$$

with

$$O_{7L,R} = \frac{em_b}{16\pi^2}\bar{s}\sigma_{\mu\nu}\frac{1 \pm \gamma_5}{2}bF^{\mu\nu}. \tag{42}$$

The subscripts L, R refer to the helicity of the emitted photon. In the $B \to K^*\gamma$ process, the K^* must have the same helicity as the emitted photon in order to

conserve angular momentum. We can write

$$\mathcal{A}(B \to K^*_{L,R}\gamma_{L,R}) \equiv C_{7L,R}\mathcal{A}^{L,R}(B \to K^*\gamma) \tag{43}$$

where

$$\mathcal{A}^{L,R}(B \to K^*\gamma) \propto \langle K^*\gamma|O_{7L,R}|B\rangle. \tag{44}$$

In this picture, the probability f_R for the emission of a right-handed photon from the b-quark is then given simply by the corresponding Wilson coefficient:

$$f_R = \frac{|\mathcal{A}(B \to K^*_R(K\gamma)\gamma_R)|^2}{|\mathcal{A}(B \to K^*(K\gamma)\gamma)|^2} = \frac{|C_{7R}|^2}{|C_{7L}|^2 + |C_{7R}|^2}$$

The naive Standard Model estimate for this fraction is $f_R \approx 0.1\%$ based on $C_{7R}/C_{7L} \approx m_s/m_b$ from the chiral structure of the W-boson couplings to quarks [8]. A recent study including other operators that contribute to $b \to s\gamma_R$ finds that f_R may be as large as 1% within the Standard Model [50].

6.3 Generalized amplitude for $B \to K^*\gamma \to K\gamma\gamma$

Let us now return to the amplitude for $B \to K^*\gamma \to K\gamma\gamma$, which was given in Eq. 33 for the Standard Model contribution arising from O_{7L} only. Following Refs. [32, 51], we can generalize this amplitude by introducing two form factors, $T_1(q^2 = 0)$ and $T_2(q^2 = 0)$:

$$\mathcal{M}_{K^*} \propto \left[T^{\mu\nu}(k_1, k_2) + T^{\nu\mu}(k_2, k_1)\right] \epsilon^*_\mu(k_1)\epsilon^*_\nu(k_2) \tag{45}$$

with

$$\begin{aligned} T^{\mu\nu}(k_1, k_2) \;=\; & C_{7L}\epsilon^{\alpha\nu\gamma\delta}k_{2\alpha}(p_B - k_1)_\gamma k_{1\beta'} \\ & \times \frac{1}{(p_B - k_1)^2 - m^2_{K^*} + im_{K^*}\Gamma_{K^*}} \left(g_{\delta\sigma'} - \frac{(p_B - k_1)_\delta (p_B - k_1)_{\sigma'}}{m^2_{K^*}}\right) \\ & \times \Big[iT_1(0)\epsilon^{\mu\beta'\sigma'\tau'}(p_B - k_1)_{\tau'} \\ & \qquad -T_2(0)\left(g^{\mu\sigma'}(p_B - k_1)^{\beta'} - g^{\beta'\sigma'}(p_B - k_1)^\mu\right)\Big], \end{aligned}$$

where we have suppressed overall constants, except C_{7L}. Examining $T^{\mu\nu}$ with respect to its symmetry properties we see immediately that the term associated with $T_1(0)$ is even under a parity transformation P (it is the product of two epsilon tensors), whereas the $T_2(0)$ term is odd (one epsilon tensor). Since both terms are invariant under charge conjugation (C), we may split $T^{\mu\nu}$ into a CP-even and a CP-odd part. This breakdown is equally valid for the full amplitude since the product of two helicity vectors is even under C and P. We may write

$$\mathcal{A}_L(B \to K^*(K\gamma)\gamma) = C_{7L}\left(T_1(0)\mathcal{A}^{\text{CP-even}} + T_2(0)\mathcal{A}^{\text{CP-odd}}\right). \tag{46}$$

It is now straightforward to construct an additional contribution describing the emission of a right-handed photon from O_7 in our amplitude, governed by the Wilson coefficient C_{7R}: application of the parity operator to turn the left-handed photon

into a right-handed one results in a sign flip of the parity-odd term, i.e. $T_2(0) \to T_2'(0) = -T_2(0)$, while $T_1(0) \to T_1'(0) = T_1(0)$. Thus we have

$$\begin{aligned}\mathcal{A}(B \to K^*(K\gamma)\gamma) &= C_{7L}\left(T_1(0)\mathcal{A}^{\text{CP-even}} + T_2(0)\mathcal{A}^{\text{CP-odd}}\right) \\ &\quad + C_{7R}\left(T_1(0)\mathcal{A}^{\text{CP-even}} - T_2(0)\mathcal{A}^{\text{CP-odd}}\right) \\ &= (C_{7L}+C_{7R})\mathcal{A}^{\text{CP-even}} + (C_{7L}-C_{7R})\mathcal{A}^{\text{CP-odd}}, \end{aligned} \quad (47)$$

where we have used $T_1(0) \approx T_2(0) = 1$ in accordance with Eq. (33) [31].

6.4 Interference with η_c and χ_{c0}

Given that the amplitude for the η_c (χ_{c0}) contribution is odd (even) under CP (Sec. 6.1), it is straightforward to rewrite the amplitude (40) in terms of CP-even and CP-odd terms:

$$\mathcal{A}(B \to K\gamma\gamma) = [\mathcal{A}_{\eta_c} + (C_{7L}-C_{7R})\mathcal{A}_{K^*}^{\text{CP-odd}}] + [\mathcal{A}_{\chi_{c0}} + (C_{7L}+C_{7R})\mathcal{A}_{K^*}^{\text{CP-even}}], \quad (48)$$

where we have neglected the non-resonant amplitude and assumed positive interference signs everywhere.

Squaring the non-interfering amplitudes before summing them up to obtain the observed decay rate, we see explicitely that the η_c–K^* interference term is proportional to $(C_{7L} - C_{7R})$ while the χ_{c0}–K^* interference term is proportional to $(C_{7L} + C_{7R})$:

$$\begin{aligned}|\mathcal{A}(B \to K\gamma\gamma)|^2 &= |\mathcal{A}_{\eta_c} + (C_{7L}-C_{7R})\mathcal{A}_{K^*}^{\text{CP-odd}}|^2 \\ &\quad + |\mathcal{A}_{\chi_{c0}} + (C_{7L}+C_{7R})\mathcal{A}_{K^*}^{\text{CP-even}}|^2 \\ &= |\mathcal{A}_{\eta_c}|^2 + |\mathcal{A}_{\chi_{c0}}|^2 + |\mathcal{A}_{K^*}|^2 \\ &\quad + (C_{7L}-C_{7R})\{\mathcal{A}_{\eta_c}\mathcal{A}_{K^*}^{\text{CP-odd}*} + \mathcal{A}_{\eta_c}^*\mathcal{A}_{K^*}^{\text{CP-odd}}\} \\ &\quad + (C_{7L}+C_{7R})\{\mathcal{A}_{\chi_{c0}}\mathcal{A}_{K^*}^{\text{CP-even}*} + \mathcal{A}_{\chi_{c0}}^*\mathcal{A}_{K^*}^{\text{CP-even}}\} \\ &= |\mathcal{A}_{\eta_c}|^2 + |\mathcal{A}_{\chi_{c0}}|^2 + |\mathcal{A}_{K^*}|^2 + (C_{7L}-C_{7R})\mathcal{I}_{\eta_c} + (C_{7L}+C_{7R})\mathcal{I}_{\chi_{c0}}, \end{aligned}$$

where $\mathcal{I}_{\eta_c,\chi_{c0}}$ are the respective intereference terms. The interference terms are accessible to experiment: they manifest themselves as enhancements or reductions in the diphoton mass spectrum of $B \to K\gamma\gamma$ decays near the resonance peaks, depending on the signs involved. The Wilson coefficients C_{7L} and C_{7R}, may thus be cleanly extracted from the observed diphoton mass spectrum, if the signs of the interference terms are known. Unfortunately, the sign of neither the η_c nor the χ_{c0} interference is known today, see Sec. 5.5, such that only values for $|C_{7L} - C_{7R}|$ and $|C_{7L} + C_{7R}|$ can be derived from a measured spectrum, leading to a four-fold ambiguity in the solution for (C_{7L}, C_{7R}). This is schematically shown in Fig. 12. In spite of the four-fold ambiguity, a measurement of these interference terms still represents a valuable test of the Standard Model. Recall that the overall normalization $|C_{7L}|^2 + |C_{7R}|^2$ is given by the inclusive $b \to s\gamma$ rate and hence already known from experiment.

Therefore the interference between the resonances contributing to $K\gamma\gamma$ is a powerful probe for measuring the Wilson coefficients C_{7L} and C_{7R}, and, in a more general sense, the photon polarization in the $b \to s\gamma$ process. In the following section, we will give a quantitative estimate of the observable effects.

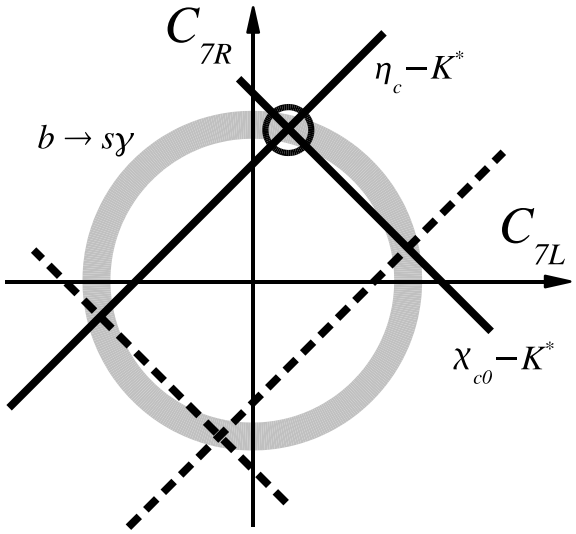

Figure 12: Schematic illustration of the constraints in the C_{7L}–C_{7R} plane obtained from a precision measurement of the diphoton mass spectrum in $B \to K\gamma\gamma$ decay. The grey circle depicts the region allowed from inclusive $b \to s\gamma$ measurements. The solid diagonal lines represent the constraints that would be obtained from the measurement of η_c–K^* and χ_{c0}–K^* interferences. In the case where the signs of the interference terms are unknown, mirror solutions appear—represented here as dashed lines—leading to the four-fold ambiguous solution for C_{7L} and C_{7R}.

6.5 Quantitative estimate of the effect

To obtain a quantitative idea of the effects to be measured, we compute diphoton mass spectra based on (40) for various values of C_{7L} and C_{7R} within the constraint on $C_{7L}^2 + C_{7R}^2$ given by the inclusive $b \to s\gamma$ rate. To simplify the notation in the following analysis, let us define the normalized Wilson coefficients $c_{7L,R} = C_{7L,R}/\sqrt{C_{7L}^2 + C_{7R}^2}$. The resulting spectra in the range of interest are shown in Fig. 13 for B^+ and B^-, where positive interference signs have been assumed throughout.

Experimentally, the interference terms are most readily isolated by means of asymmetries. An observable that is particularly convenient to extract the η_c interference is the charge asymmetry A_C, defined as

$$A_C(m_{\gamma\gamma}) = \frac{d\Gamma(B^- \to K^-\gamma\gamma)/dm_{\gamma\gamma} - d\Gamma(B^+ \to K^+\gamma\gamma)/dm_{\gamma\gamma}}{d\Gamma(B^- \to K^-\gamma\gamma)/dm_{\gamma\gamma} + d\Gamma(B^+ \to K^+\gamma\gamma)/dm_{\gamma\gamma}}. \qquad (49)$$

A completely analog asymmetry may be defined for neutral B decays, but its experimental observation will be hampered by the difficulty of tagging the flavor of the B meson. This is in part compensated by the larger branching fraction for the neutral decay chain. For simplicity, however, we will restrict our analysis to the charged decay. Note that the charge asymmetry A_C is not a CP-asymmetry; it simply compensates the parity violation introduced by the photon helicity to ensure CP conservation, as expected to first order in the Standard Model. In Fig. 14 we show

the expected A_C for the relevant diphoton mass range, for various combinations of c_{7L} and c_{7R}. It exhibits the typical shape of a Breit-Wigner interference around the position of the η_c resonance, with a distortion at higher energies due to the presence of the χ_{c0} resonance, which forces the charge asymmetry to zero in its vicinity. The positions of maximum asymmetry are given by the relative strength of the η_c and K^* resonance contributions. With our branching fractions, (36) and Table 3, we find maximum asymmetry some ten (check numerically with box assumption for K^*, and Breit-Wigner for η_c!) resonance widths Γ_{η_c} away from the peak. The value of the maximum asymmetry is a direct measure of $(c_{7L} - c_{7R})$. If we restrict the analysis to the region below the η_c peak (to avoid distoritions due to the χ_c resonance) we find that the maximum asymmetry $A_C^{\max}$, positive or negative, obeys the proportionality

$$A_C^{\max} \approx 0.37(c_{7L} - c_{7R}) \qquad (m_{\gamma\gamma} < m_{\eta_c}). \tag{50}$$

In the absence of any knowledge on the interference sign, only the modulus of $(c_{7L} - c_{7R})$ is determined.

The χ_{c0} interference, being CP-even, cannot be extracted in the same manner: the resulting spectra are the same for B^+ and B^-. A charge-averaged peak asymmetry around the χ_{c0} may be used in this case to extract the interference. Let us define

$$A_{\chi_{c0}}(\Delta m_{\gamma\gamma}) = \frac{d\overline{\Gamma}(m_{\chi_{c0}} - \Delta m_{\gamma\gamma})/dm_{\gamma\gamma} - d\overline{\Gamma}(m_{\chi_{c0}} + \Delta m_{\gamma\gamma})/dm_{\gamma\gamma}}{d\overline{\Gamma}(m_{\chi_{c0}} - \Delta m_{\gamma\gamma})/dm_{\gamma\gamma} + d\overline{\Gamma}(m_{\chi_{c0}} + \Delta m_{\gamma\gamma})/dm_{\gamma\gamma}}, \tag{51}$$

where $\overline{\Gamma}$ denotes the charge-averaged decay rate,

$$\overline{\Gamma} = \frac{\Gamma(B^+ \to K^+\gamma\gamma) + \Gamma(B^- \to K^-\gamma\gamma)}{2}. \tag{52}$$

The expected peak asymmetry is shown in Figure 15, again for various combinations of c_{7L} and c_{7R}. Since the distribution of $B \to K^*(K\gamma)\gamma$ events is rather flat in that region, the peak asymmetry is dominated by the interference effect we wish to extract. With our branching ratio assumptions the maximum peak asymmetry $A_{\chi_{c0}}^{\max}$ (positive of negative) is found at some 50 MeV from the χ_{c0} peak, well before the η_c resonance on the low-mass side starts to push the asymmetry towards one. As expected, for this asymmetry we find that the maximum value is proportional to $c_{7L} + c_{7R}$). Indeed, we have

$$A_{\chi_{c0}}^{\max} \approx 0.40(c_{7L} + c_{7R}), \tag{53}$$

in analogy to (50). As in the case of A_C, ignorance of the interference sign means that only the absolute value of $(c_{7L} + c_{7R})$ is measured.

The combined measurement of $A_C^{\max}$ and $A_{\chi_{c0}}^{\max}$ would give the four-fold ambiguous solution depicted in Fig. 12. An optimal extraction of the Wilson coefficients from experimental data would proceed via an unbinned maximum-likelihood analysis of the observed population across the entire Dalitz plot. We show the suggested asymmetries here simply in order to illustrate the potential of our method.

6.6 Experimental considerations

We have shown that in principle information on the Wilson coefficients C_{7L} and C_{7R} can be obtained from the diphoton spectrum obtained from $B \to K\gamma\gamma$. Let us now briefly touch on the experimental prospects for measuring the required asymmetries.

In terms of statistics the limiting factor for observing the required interference terms is the number of $B \to K^*\gamma \to K\gamma\gamma$ decays underneath the resonance peaks. From our generated spectra we infer that at least of the order of 10^3 clean $B \to K^*\gamma \to K\gamma\gamma$ decays would be needed to observe asymmetries allowing the discrimination between the case of a fully polarized and that of an unpolarized photon emitted in the $b \to s\gamma$ process.

With the branching fractions (35) and (36) this corresponds to several 10^9 neutral or charged B mesons to be produced and detected. Reconstruction efficiencies for radiative decay channels are of the order of 10% at B factories [22, 23]. At hadron colliders, the expected overall trigger and reconstruction efficiencies for radiative decays are of the order of 0.1%, if the decay features a vertex formed by two charged tracks [52]. Triggering on just one displaced track identified as a kaon, in addition to the high-transverse-momentum photons and the properties of the accompanying B, may prove difficult but not impossible.

Thus a measurement of the suggested asymmetries would require the production of several 10^{10} B mesons in the case of an e^+e^- B factory. This falls in the range of the proposed "Super-B factories" [17, 18], where initial performance estimates were carried out assuming the production of up to 5×10^{10} B mesons of each of the charged and neutral type.

At a hadron collider, the corresponding estimate amounts to about 10^{12} B mesons, corresponding to the expected annual $B^\pm$ production rate at the LHCb experiment [52]. Therefore, at least from the statistical point of view, the measurement appears feasible, in particular if one takes into consideration the possibility of a luminosity upgrade.

Many other experimental issues will play a role in such a measurement, such as photon energy resolution and bias due to electromagnetic shower leakage and of course backgrounds due to physics, instrumental and combinatorial effects. These issues can only be addressed within the context of a specific experimental setup and with more knowledge on the physics of the amplitudes involved in $B \to K\gamma\gamma$ decay (higher kaon resonances for instance).

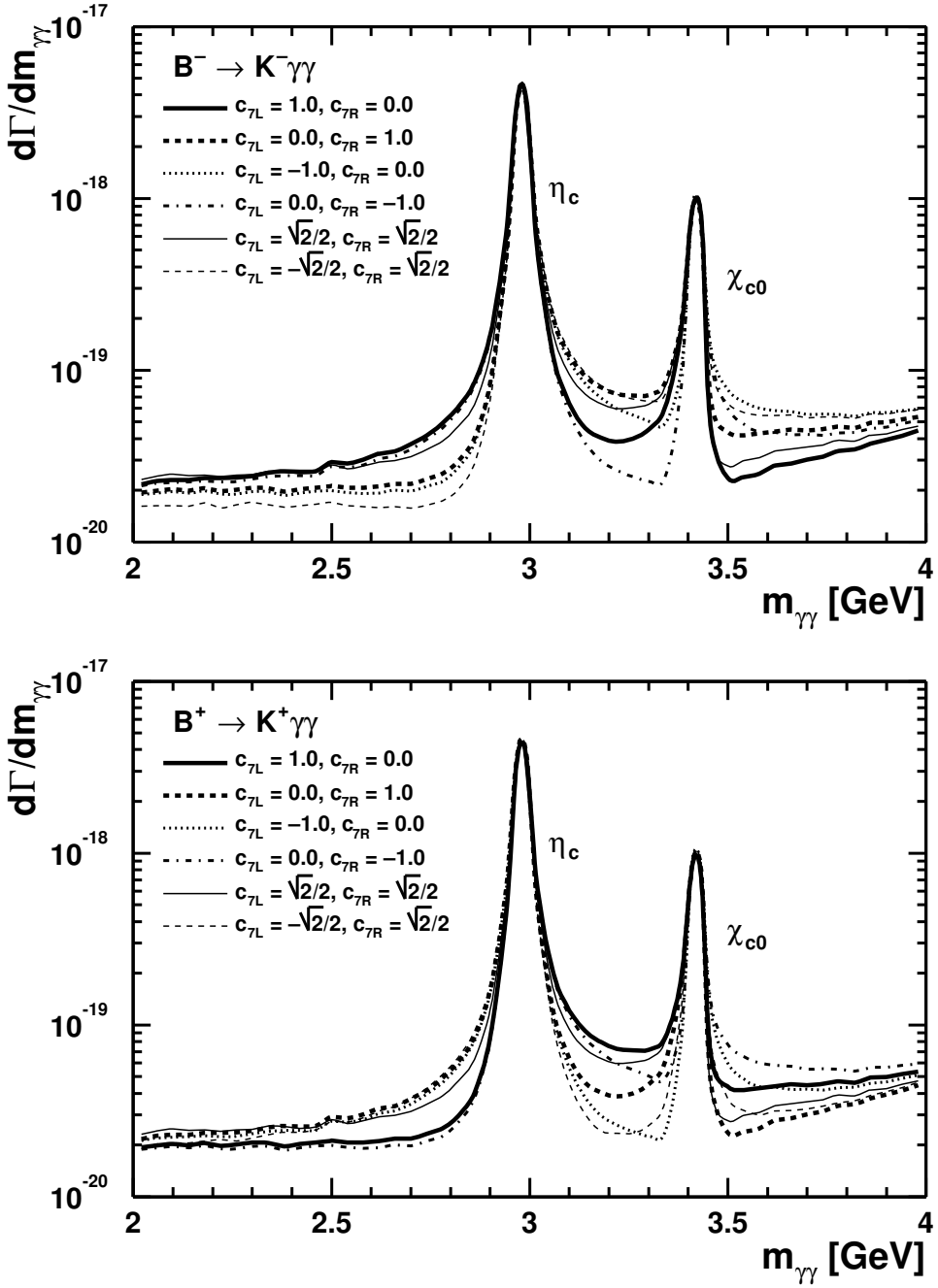

Figure 13: Diphoton mass spectra for various values of the normalized Wilson coefficients c_{7L} and c_{7R} (see text). Top: $B^- \to K^-\gamma\gamma$, bottom: $B^+ \to K^+\gamma\gamma$. All interference terms are assumed to have positive sign.

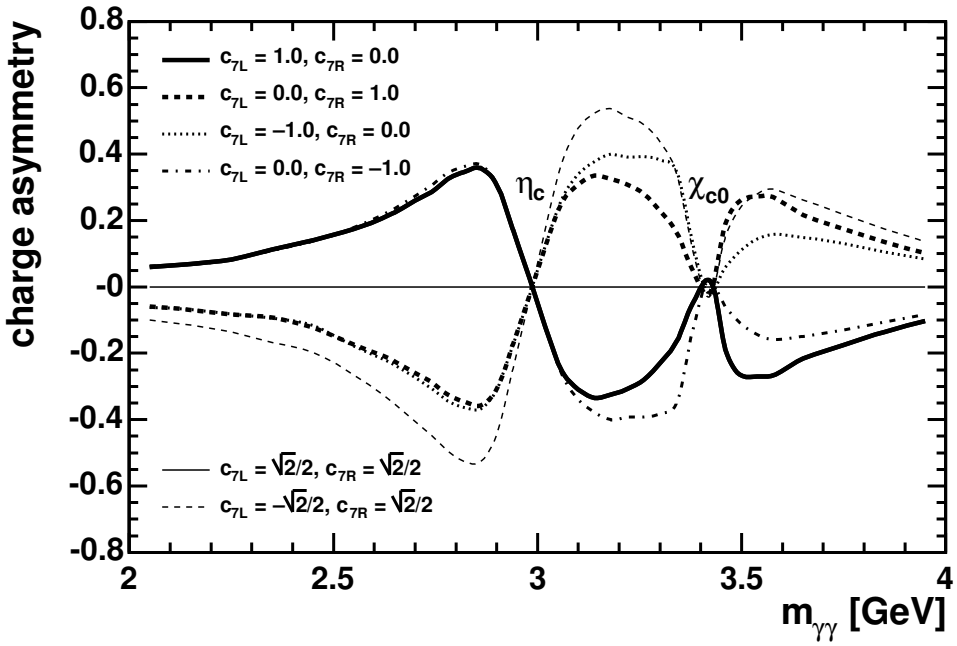

Figure 14: Charge asymmetry A_C as a function of the diphoton mass for various values of the normalized Wilson coefficients c_{7L} and c_{7R}. All interference terms are assumed to have positive sign.

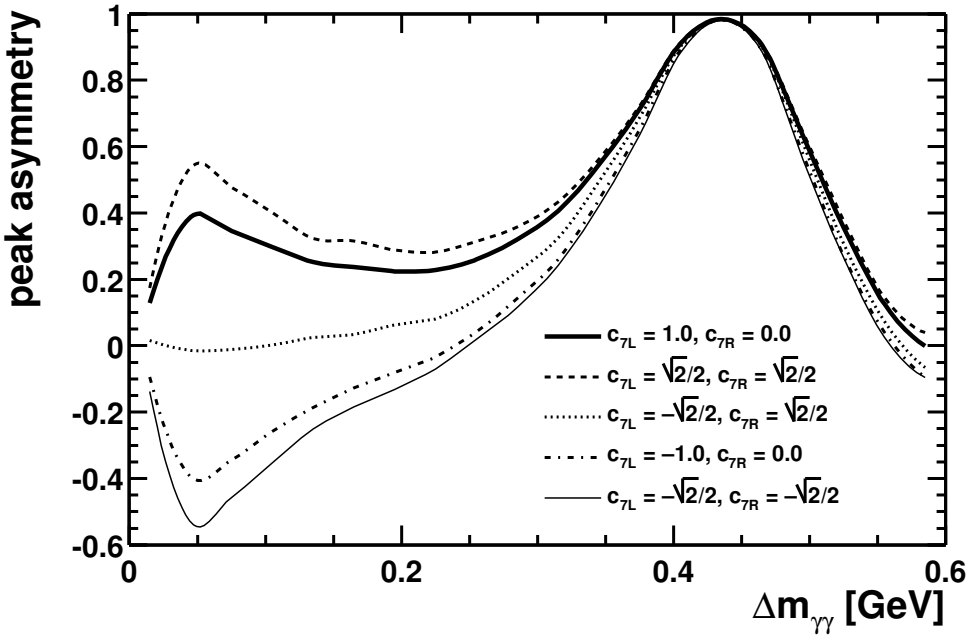

Figure 15: Peak asymmetry $A_{\chi_{c0}}(m_{\gamma\gamma})$ for various values of the normalized Wilson coefficients c_{7L} and c_{7R}. All interference terms are assumed to have positive sign.

7 Summary

Our main conclusion is that contributions to $B \to K\gamma\gamma$ from kaon resonances are sizeable and may turn out to be useful in the search for or the investigation of physics beyond the Standard Model.

Based on the measured branching fractions for $B \to K^*\gamma$ and $K^* \to K\gamma$ and the Standard Model amplitude for the cascade decay we find that the total branching fraction due to $B \to K^*\gamma \to K\gamma\gamma$ amounts to about 3.5 (1.5) $\times 10^{-7}$ for the neutral (charged) decay, thanks to a substantial enhancement from the interference term between the two photon-exchanged amplitudes. This same interference term also brings about a non-negligible fraction of decays with photon energies far from the K^* resonance peaks. This contribution is present throughout the phase space (Dalitz plot) of the $B \to K\gamma\gamma$ decay. Estimated to be at least an order of magnitude larger than the short-distance (non-resonant) Standard Model contribution at any point in phase space, it renders the latter completely inaccessible to experiment. Since these kaon resonance contributions are present in all decays to a strange hadronic system and two photons, we must conclude that $B \to X_s\gamma\gamma$ is unsuitable to study the fundamental quark transition $b \to s\gamma\gamma$. The only hope to observe this process is the exclusive decay $B_s \to \gamma\gamma$.

Several other kaon resonances are known to contribute to the $K\gamma\gamma$ final state at comparable strength, such that the overall $K\gamma\gamma$ branching fraction from $B \to K_{\rm res}\gamma$ may well exceed 10^{-6} and therefore be accessible already at current B meson facilities.

In the long run, the detailed study of interferences between decays via kaon and charmonium resonances gives access to the helicity of the photon emitted in the $b \to s\gamma$ transition, which represents an important test of the Standard Model. We have found that such a measurement is within the statistical reach of proposed and planned B experiments at e^+e^- and hadron colliders. While this method to determine the photon polarization in $b \to s\gamma$ decay requires more statistics than the more conventional ones, it has the advantage that it yields additional information on the Wilson coefficients C_{7L} and C_{7R}.

References

[1] S. Chen et al. (CLEO Collaboration), Phys. Rev. Lett. **87** (2001) 251807; P. Koppenburg et al. (Belle Collaboration), Phys. Rev. Lett. **93** (2004) 061803.

[2] See, for instance, T. Hurth, Rev. Mod. Phys. **75** (2003) 1159.

[3] L. Reina, G. Ricciardi, A. Soni, Phys. Lett. B **396** (1997) 231.

[4] L. Reina, G. Ricciardi, A. Soni, Phys. Rev. D **56** (1997) 5805.

[5] J. Cao, Z. Xiao, G. Lu, Phys. Rev. D **64** (2001) 014012.

[6] A. Gemintern, S. Bar-Shalom, G. Eilam, Phys. Rev. D **70** (2004) 035008.

[7] G. Hiller, A.S. Safir, J. High Energy Phys. JHEP02 (2005) 011.

[8] D. Atwood, M. Gronau, A. Soni, Phys. Rev. Lett. **79** (1997) 185.

[9] B. Aubert et al. (BABAR Collaboration), Phys. Rev. Lett. **93** (2004) 201801; Y. Ushiroda et al. (Belle Collaboration), to be submitted to Phys. Rev. Lett.

[10] Y. Grossman, D. Pirjol, J. High Energy Phys. **06** (2000) 029.

[11] D. Melikhov, N. Nikitin, and S. Simula, Phys. Lett. B **442** (1998) 381.

[12] M. Gronau, Y. Grossman, D. Pirjol, A. Ryd, Phys. Rev. Lett. **88** (2002) 051802.

[13] M. Gronau, D. Pirjol, Phys. Rev. D **66** (2002) 054008.

[14] T. Mannel, S. Recksiegel, Acta Phys. Polon. B **28** (1997) 2489; J. Phys. G: Nucl. Part. Phys. **24** (1998) 979.

[15] G. Hiller, A. Kagan, Phys. Rev. D **65** (2002) 074038.

[16] F. Legger, T.Schietinger, hep-ph/0605245, submitted to Phys. Lett. B.

[17] S. Hashimoto, M. Hazumi, J. Haba, J.W. Flanagan, and Y. Ohnishi (eds.), *Letter of Intent for KEK Super B Factory*, KEK Report 2004-4 (2004).

[18] J. Hewett, D.G. Hitlin (eds.), *The Discovery Potential of a Super B Factory, Proceedings of the 2003 SLAC Workshops*, SLAC-R-709 (2004).

[19] F. Gianotti et al., Eur. Phys. J. C **39** (2005) 293.

[20] M. Knecht, T. Schietinger, Phys. Lett. B 634 (2006) 403.

[21] R. Ammar et al. (CLEO Collaboration), Phys. Rev. Lett. **71** (1993) 674.

[22] M. Nakao et al. (Belle collaboration) Phys. Rev. D **69** (2004) 112001.

[23] B. Aubert et al. (BABAR collaboration), Phys. Rev. Lett. **88** (2002) 101805.

[24] J. Alexander et al. (Heavy Flavor Averaging Group), *Averages of b-hadron Properties as of Summer 2004*, hep-ex/0412073, unpublished, and April 2005 web update available at `http://http://www.slac.stanford.edu/xorg/hfag`

[25] D. Carlsmith et al., Phys. Rev. Lett. **56** (1986) 18.

[26] S. Eidelman et al. (Particle Data Group), Phys. Lett. B **592** (2004) 1.

[27] C. Chandlee et al., Phys. Rev. Lett. **51** (1983) 168.

[28] D.M. Berg ,*Measurement of the radiative decay width of the negative K^*-meson*, FERMILAB-THESIS-1983-15, UMI-83-21652 (unpublished).

[29] P.J. O'Donnell, Rev. Mod. Phys. **53**, (1981) 673; G. Morpurgo, Phys. Rev. D **42** (1990) 1497; M. Benayoun, L. DelBuono, S. Eidelman, V.N. Ivanchenko, and H.B. O'Connell, Phys. Rev. D **59** (1999) 114027.

[30] J. Richman, *An experimenter's guide to the helicity formalism*, CALT-68-1148 (unpublished).

[31] S.R. Choudhury, G.C. Joshi, N. Mahajan, B.H.J. McKellar, Phys. Rev. D **67** (2003) 074016.

[32] P. Singer, D.X. Zhang, Phys. Rev. D **56** (1997) 4274.

[33] D. Lange, A. Ryd, *The EvtGen event generator package*, International Conference on Computing in High Energy Physics, Chicago, Illinois, USA, August 31–September 4, 1998.

[34] M. Knecht, LPHE note 2004-014 (unpublished), available at `http://lphe/publications/2004/lphe_2004_14.pdf`.

[35] S.J. Richichi et al. (CLEO Collaboration), Phys. Rev. Lett. **85** (2000) 520; H. Aihara (for the Belle Collaboration), talk given at the conference on Flavor Physics and CP Violation, 3–6 June 2003, Paris; P. Chang et al. (Belle Collaboration), hep-ex/0412043 (submitted to Phys. Rev. D); B. Aubert et al. (BABAR Collaboration), hep-ex/0502017 (submitted to Phys. Rev. Lett.); B. Aubert et al. (BABAR Collaboration), hep-ex/0503035 (submitted to Phys. Rev. Lett.).

[36] S. Cihangir et al. (Fermilab-Minnesota-Rochester Collaboration), Phys. Lett. B **117** (1982) 123.

[37] S. Nishida et al. (Belle Collaboration), Phys. Rev. Lett. **89** (2002) 231801; B. Aubert et al. (BABAR Collaboration), Phys. Rev. D **70** (2004) 091105; Heyoung Yang et al. (Belle Collaboration), Phys. Rev. Lett. **94** (2005) 111802.

[38] A. Alavi-Harati et al. (KTeV Collaboration), Phys. Rev. Lett. **89** (2002) 072001.

[39] K.W. Edwards et al. (CLEO Collaboration), Phys. Rev. Lett. **86** (2001) 30.

[40] F. Fang et al. (Belle Collaboration), Phys. Rev. Lett. **90** (2003) 071801.

[41] K. Abe et al. (Belle Collaboration), Phys. Rev. Lett. **88** (2002) 031802.

[42] B. Aubert et al. (BABAR Collaboration), Phys. Rev. D **69** (2004) 071103; Phys. Rev. Lett. **94** (2005) 171801.

[43] C. Meng, Y.-J. Gao, K.-T. Chao, hep-ph/0502240.

[44] S.-K. Choi et al. (Belle Collaboration), Phys. Rev. Lett. **89** (2002) 102001.

[45] S.R. Choudhury, G.C. Joshi, N. Mahajan, B.H.J. McKellar, Phys. Rev. D **72** (2005) 119906.

[46] P.J. O'Donnell, H.K.K. Tung, Phys. Rev. D **43** (1991) 2067.

[47] S. Mantry, D. Pirjol, I.W. Stewart, Phys. Rev. D 68 (2003) 114009.

[48] See, for instance, A.J. Buras, R. Fleischer, S. Recksiegel, F. Schwab, Phys. Rev. Lett. 92 (2004) 101804.

[49] C.N. Yang, Phys. Rev. **77** (1950) 242.

[50] B. Grinstein, Y. Grossman, Z. Ligeti, and D. Pirjol, Phys. Rev. D **71** (2005) 011504.

[51] P. Singer, Phys. Rev. D **49** (1994) 7.

[52] R. Antunes Nobrega et al. (LHCb Collaboration), *LHCb Reoptimized Detector Design and Performance Technical Design Report*, CERN/LHCC 2003-030.